Article

Not peer-reviewed version

Puerariae Lobatae Radix Alleviates High Salt Diet Induced Chronic Kidney Disease by Repairing Intestinal Epithelial Barrier and Down-Regulating Fibrotic Signaling

Peng Wu *, Jingwen Xue, Zhangrui Zhu, Yao Yu, Qi Sun, Ming Xie, Benlin Wang, Pengcheng Huang, Zhengyuan Feng, Jie Zhao *

Posted Date: 3 January 2024

doi: 10.20944/preprints202401.0241.v1

Keywords: Puerariae Lobatae Radix; High salt diet; Chronic kidney disease; Wnt / β-catenin pathway; Gut microbiota; Fecal microbiota transplantation

Article

Puerariae Lobatae Radix Alleviates High Salt Diet Induced Chronic Kidney Disease by Repairing Intestinal Epithelial Barrier and Down-Regulating Fibrotic Signaling

Peng Wu [1,†,*], Jingwen Xue [1,†], Zhangrui Zhu [1,†], Yao Yu [1], Qi Sun [1], Ming Xie [1], Benlin Wang [1], Pengcheng Huang [1], Zhengyuan Feng [1] and Jie Zhao [2,*]

[1] Department of Urology, Nanfang Hospital, Southern Medical University, 510515, PR China
[2] NMPA Key Laboratory for Research and Evaluation of Drug Metabolism, Guangdong Provincial Key Laboratory of New Drug Screening, School of Pharmaceutical Sciences, Southern Medical University, Guangzhou 510515, PR China
* Correspondence: doctorwupeng@gmail.com (P. Wu), zhaojie_0412@163.com (J. Zhao).
† These authors contributed equally to this work.

Abstract: Chronic kidney disease (CKD) progression can be accelerated by excessive sodium consumption. Gut microbiota dysfunction is a key factor affecting high salt related kidney disease susceptibility. *Puerariae Lobatae* Radix (PLR), a traditional Chinese medicine and food homologous herb, is known to promote gut microbiota homeostasis, however, its role in renoprotection remains unknown. This study aimed to investigate the efficacy and potential mechanism of PLR to alleviate CKD. An 8-week 2% NaCl-feeding murine model was applied to induce CKD and evaluate the therapeutic effect of PLR supplementary. After gavage for 8 weeks, PLR significantly alleviated CKD-associated creatinine, urine protein increasement and nephritic histopathological injury. Moreover, PLR protected kidney from fibrosis by down-regulating inflammatory response and the canonical Wnt / β-catenin pathway. Further, we found PLR rescued gut microbiota dysbiosis and protected high salt-induced gut barrier dysfunction. We found enrichment of *Akkermansia* and *Bifidobacterium* after PLR intervention, the relative abundance of which were in positive correlation with normal maintenance of renal histology and function. Next, fecal microbiota transplantation experiment verified that microbiota from mice treated with PLR could ameliorated kidney tissue injury and intestinal barrier damage. Thus, the positive effect of PLR on CKD was at least partially exerted through gut microbiota reestablishment and down-regulation of the Wnt / β-catenin pathway. Our study provides evidence for new function of PLR on kidney protection and put forward a potential therapeutic strategy target for CKD.

Keywords: *Puerariae Lobatae* Radix; high salt diet; Chronic kidney disease; Wnt / β-catenin pathway; gut microbiota; fecal microbiota transplantation

1. Introduction

Chronic kidney disease (CKD), a slowly progressive and irreversible kidney function failure, affected approximately 10% of global population[1]. Ascending clinical evidence suggests that excessive sodium intake accelerate the progression of CKD and relevant hypertension[2,3]. Besides, high level of sodium had been proved to induce kidney cytokine expression as well as tissue regeneration and fibrosis by activating Wnt / β-catenin and TGF-β signaling[4–6]. It follows that excessive sodium intake is one of the important risk factors for CKD progression. Besides advocating salt reduction, it is critical to explore remedy to reconcile the adverse impact of excessive sodium consumption on CKD.

Intestine has a rich and structurally diverse intestinal microbiome that engaged in multiple interactions affecting host health by influencing the intrinsic immunity and metabolism. Moreover,

 doi:10.20944/preprints202401.0241.v1

the composition and function of the gut microbiota is dynamic and easily affected by diet properties. By importing dietary element into the bond between the host and its microbiota, nutrition maintains homeostasis or leads to disease susceptibility[7]. As one of the most essential dietary components, excessive salt intake has been extensively studied and proven to cause a wide range of diseases through its effects on gut microbiome[8]. Previous studied have shown that consumption of high salt resulted in alteration of gut microbiota structure that may be pro-inflammatory to exacerbates colitis and hypertension[9,10]. High salt induced gut barrier disruption triggers renal function injury[11]. These indicated that excessive salt intake could cause susceptibility of a wide range of diseases through gut microbiome. Moreover, depletion of gut microbiome or administering probiotics can ease the progression of many diseases[11,12]. Together, this provides us with ideas to reverse progression of high salt related CKD through regulation of gut microbiome.

Puerariae Lobatae Radix (PLR) is rich in nutrients including flavonoids, starch, saponins, and amino acids, and has always been a medicine and food homologous herb to relieve gastrointestinal and cardiovascular diseases[13]. Multiple studies have indicated that PLR and its active ingredient might alleviate diabetes related kidney damage and nonalcoholic fatty liver disease through modulating gut microbiota[14,15]. In our previous study, we also confirmed PLR promoted gut microbiota homeostasis, increased the relative abundance of beneficial bacteria and protected the structural and functional integrity of the gut barrier, blood-brain barrier, and placental barrier, thus contributed to vascular anomalies related diseases including ischemic stroke and pre-eclampsia[13,16]. CKD is a disease closely related to host metabolic disorder and vascular dysfunction, bioflavonoids and other bioactive compound have been verified to relieve CKD associated biochemical abnormalities and kidney inflammation[17], however, few studies have focused on whether PLR exerts a protective effect on it.

In this study, we constructed a high salt induced CKD murine model and investigated the renoprotective effects of PLR. We found that PLR alleviated high salt diet induced CKD by repairing intestinal epithelial barrier and down-regulating fibrotic signaling. In addition, this protective effect was exerted, at least partly by promoting homeostasis of gut microbiota.

2. Materials and Methods

2.1. Source and preparation of PLR decoction

Medicinal slices form of PLR were purchased from Guangzhou Weida Company (Guangzhou, China). Standard substance of *puerarin* (purity ≥ 99.0%), *daidzin* (purity ≥ 98.0%) and *daidzein* (purity ≥ 98.0%) were purchased from Chengdu Must Bio-Technology Company (Chengdu, Sichuan, China). PLR decoction preparation was conducted as previously described[13,16]. In brief, take a certain quality of PLR and extract in boiling distilled water at a ratio of 1:10 (*w*/*v*) for 1 hour, collect the filtrate and boiling the residue with distilled water (1:6, *w*/*v*) for another 1 hour. Concentrate the above filtrates and quantify the content of *puerarin*, *daidzin*, and *daidzein* by using ultra-performance liquid chromatography (specific method is listed in Supplementary Table S1 and Figure S1). Organic phase methanol was obtained from Tianjin Da Mao chemical reagents factory (Tianjin, China). The respectively concentrations of these three compounds were 10.9, 17.5, and 0.3 mg/mL.

2.2. Animals and experimental design

All animal experimental procedures were conducted in strict accordance with the National Institute of Health guidelines and were approved by the Institutional Animal Ethical Care Committee of Southern Medical University (Guangzhou, China), Reference number: NFYY-2021-0572. Specific pathogen free male C57BL/6 mice (6-8 week, weighing 20-24 g) were purchased from SPF Biotechnology Co., Ltd. (Beijing, China). All mice were housed under standard conditions of temperature and humidity with a 12h: 12h light-dark cycle and free access to food and water. After one week of acclimatization, high salt feeding mice were given drinking water containing 2% (*w*/*v*) NaCl for 8 weeks as described in previous study[11] (HS, $n = 6$), while PLR intervention mice received *Pueraria* decoction (containing 18 mg/kg, 36 mg/kg and 72 mg/kg *Puerarin*, respectively) by oral

 doi:10.20944/preprints202401.0241.v1

gavage once a day along with 8 weeks high salt feeding (PLR-L, PLR-M and PLR-H, $n = 6$ per group). Control mice receive normal drinking water during the experiment (CON, $n = 6$). There were no differences in baseline covariates among groups. And the feces and urine were collected every week for further examination. Mice were sacrificed under anesthesia and blood, kidney, liver, spleen, colon and cecal contents samples were harvested in a sterile manner for further analysis.

For blood pressure measurement, systolic blood pressure (SBP) and mean blood pressure (MBP) were measured every week via non-invasive tail cuff method, using a BP-2010A instrument (Softron Biotechnology, Beijing, China). All measurements were operated between 8am to 12am. At least six continuous stable results of each mouse were obtained and calculated the average value as the final result.

2.3. Fecal microbiota transplantation (FMT) experiment

FMT experiment was performed based on the modified method previously described[11]. In brief, feces from the donor mice (HS and PLR-H group mice) were collected in aseptic centrifugal tubes respectively and resuspended in PBS at 125 mg/mL, the mixtures were centrifuged at 1000×g for 1 min and the supernatants were collected and saved in separate 1.5 mL tubes for subsequently microbiota transplantation. Before FMT experiment, the acceptor male C57BL/6 mice (6-8 week) were given antibiotics (ABX) (vancomycin, 100 mg/kg; neomycin sulfate 200 mg/kg; metronidazole 200 mg/kg; and ampicillin 200 mg/kg) intragastrically once a day for 1 w to deplete the gut microbiota. All the mice then received drinking water containing 2% (*w*/*v*) NaCl for 8 weeks as above described. An amount of 150 μL of the fecal microbiota solution was simultaneously orally gavaged to mice once a day in the first 2 weeks, every other day in the following 2 weeks and twice each week in the last 4 weeks. The mice that received feces from HS mice or PLR-L group mice were referred to as HS-FMT group or PLR-FMT group ($n = 8$ per group). Control mice receive normal drinking water during the experiment (CON, $n = 5$). Blood pressures were measured as above described every week. All the mice had free access to food and water, and the feces and urine were collected before sacrifice. Mice were sacrificed under anesthesia and then blood, kidney, liver, spleen, colon and cecal contents samples were harvested in a sterile manner for further analysis.

2.4.16. S rDNA gene sequencing and microbe analysis

Feces were collected in sterilized 1.5 mL tubes and frozen at -80 ℃ before DNA extraction. Microbial DNA from fecal samples were extracted as previously described[18,19]. V3-V4 region of 16S rDNA was amplified by PCR using the below primers (341F, 5′-CCTACGGGNGGCWGCAG-3′ and 806R, 5′-GGACTACHVGGGTATCTAAT-3′). Amplicons were purified using the AxyPrep DNA Gel Extraction Kit (Axygen Biosciences, Union City, CA, U.S.). Purified amplicons were pooled in equimolar and paired end sequenced (PE250) on an Illumina platform according to the standard protocols. Alpha diversity were calculated in QIIME [20](version 1.9.1). PCoA and NMDS of weighted unifrac distances were generated in R project Vegan package (version 2.5.3). Biomarker features in each group were screened by LEfSe software[21] (version 1.0). The KEGG pathway analysis of the OTUs was inferred using Tax4Fun[22] (version 1.0) and were generated using Omicsmart, a dynamic real-time interactive online platform for data analysis (http://www.omicsmart.com). Pearson correlation coefficient between environmental factors and species was calculated in R project psych package (version 1.8.4) then generated using the Wekemo Bioincloud (https:// www.bioincloud.tech). The calculated p value was gone through FDR correction, taking FDR ≤ 0.05 as a threshold.

2.5. RNA-seq analysis

Kidney samples were collected in sterilized 1.5 mL tubes and frozen at -80℃ before DNA extraction. Total RNA was extracted using the EastepTM Super Total RNA Extraction Kit (Promega Corporation, Madison, WI, USA) according to the manufacturer's instructions. After total RNA was extracted, eukaryotic mRNA was enriched by Oligo(dT) beads. Then fragments were transcribed into

 doi:10.20944/preprints202401.0241.v1

cDNA by using NEBNext Ultra RNA Library Prep Kit for Illumina (NEB #7530, New England Biolabs, Ipswich, MA, USA). The ligation reaction was purified and PCR amplified. The resulting cDNA library was sequenced using Illumina Novaseq6000 by Gene Denovo Biotechnology Co. (Guangzhou, China). RNAs differential expression analysis was performed by DESeq2[23] software between two different groups. The transcripts with the parameter of false discovery rate (FDR) below 0.05 and absolute fold change ≥ 2 were considered differentially expressed transcripts. Gene set enrichment analysis (GSEA) was performed using software GSEA[24] and MSigDB[24] to identify whether a set of genes in specific KEGG pathway shows significant differences in two groups.

2.6. Gene expression analysis

Total RNA was extracted from kidney and colon tissue using the Animal Total RNA Isolation Kit (Foregene Co., Ltd, Chengdu, China) according to the manufacturer's instructions. A reverse transcript enzyme, HiScript III RT SuperMix for qPCR (+gDNA wiper) (Vazyme Biotech Co., Ltd, Nanjing, China) was applied to obtain cDNA. The real-time quantitative PCR reactions were performed on the LightCycler480 (Roche Diagnostics International, Rotkreuz, Switzerland) using a ChamQ SYBR qPCR Master Mix (Vazyme, Nanjing, China). Relative quantification of target genes were calculated using the $2^{-\triangle\triangle CT}$ method. *Gapdh* was used as a control gene. All the target gene primer sequences are listed in Supplementary Table S2.

2.7. Protein expression and biochemical analysis

The kidney and colon tissue protein were extracted with a commercial RIPA lysis buffer (Epizyme Biomedical Technology Co., Ltd, Shanghai, China) adding 1% cocktail protease inhibitor (Meilunbio, Dalian, China). Western blot was performed with the primary antibodies for Occludin, ZO-1 (Abcam, Cambridge, MA, USA), Claudin-1, TNF-α, IL-1β (ImmunoWay, Suzhou, China), β-catenin (Proteintech, Wuhan, China) and β-actin (Beijing Ray Antibody Biotech, Beijing, China). Serum creatinine was determined by using a creatinine (Cr) Assay kit (sarcosine oxidase) (Nanjing Jiancheng Bioengineering institution Co., Ltd, Nanjing, China). The urinary protein, serum LPS and serum TNF-α level were detected manually with commercial ELISA Kit (MEIMIAN, Yancheng, China). Serum and urine Na^+ concentrations were determined on an automatic biomedical analyzer (Roche Diagnostics International, Rotkreuz, Switzerland).

2.8. FD-4 permeability experiment

FITC Dextran 4-KD (FD-4, Sigma, Shanghai, China) was used to detect intestinal permeability *in vivo*. FD-4 was orally administered to mice at a dose of 0.6 mg/kg four hours before serum was harvested. The FD-4 level in serum was detected keep in the dark, based on a standard curve and spectrofluorometrically with an excitation wavelength of 485 nm and an emission wavelength of 530 nm in a microplate fluorescence reader (Infinite® M1000 PRO, TECAN, Switzerland).

2.9. Imaging of intestinal inflammation in vivo

L-012 (FUJIFILM Wako Pure Chemical corporation, Tokyo, Japan) was used to confirm intestinal inflammation *in vivo*[25]. The mice were anesthetized in an anesthesia chamber with 1.5–2.0% isoflurane–mixed gas and injected with 100 μL of a 20-mmol L-012 solution. 1 min later, IVIS Spectrum CT system was used to acquire bioluminescent images. For postacquisition analysis, the Living Image software was used to quantify the bioluminescent signals at standardized regions of interest (ROIs) defined on the abdomen.

2.10. Histological staining and analysis

The left kidney and colon tissue of mice were collected and fixed in 4% paraformaldehyde. The samples were then embedded in paraffin, sectioned at 4 μm thick and stained with hematoxylin and eosin (HE) or Masson's trichrome. The kidney tissue histological damage was accessed according to previously described scoring method[26]. The kidney fibrosis area was selected randomly from at

 doi:10.20944/preprints202401.0241.v1

least 5 points of cortical fields and quantified using image J software. Immunohistochemistry was performed using the primary antibodies for Occludin, ZO-1 (Abcam, Cambridge, MA, USA), Claudin-1 (ImmunoWay, Suzhou, China). Quantification of the average optical density was performed by automated image analysis in five randomly chosen × 200 fields of each sample. All images were scanned by a NanoZoomer Digital slide scanner and captured at × 200 or × 400 with an NDP. View2 Plus Image viewing software (Hamamatsu Photonics, Hamamatsu, Japan).

2.11. Immunofluorescence

Colon paraffin section samples were generated as above described, blocked for 1 h, and incubated at 4 °C with anti-β-catenin antibody (Proteintech, Wuhan, China) overnight. Then the slices were washed and stained with DAPI for 10 min. Images were captured with fluorescent microscopy (Olympus, Japan). Quantification of the fluorescence intensity was calculated by automated image analysis in five randomly chosen × 200 fields of each sample.

2.12. Statistical analysis

Results were represented as means ± standard error of the mean (SEM) and performed using GraphPad Prism software (version 8.0) (GraphPad Software, San Diego, Canada). Statistical analyses were performed using one-way analysis of variance (ANOVA) or repeated measurement ANOVA as indicated in the figure legends. A p-value < 0.05 was considered statistically significant.

3. Results

3.1. PLR alleviated CKD and renal fibrosis induced by high salt diet

To investigate whether therapeutic PLR administration can have an impact on kidney injury induced by high salt diet, we adopted an 8-week intake of high salt murine model to induce CKD and provide them with low, middle and high dose of PLR to evaluate its effect. CKD is often accompanied by elevated blood pressure; therefore, we monitored the dynamic blood pressure changes. There were no differences in baseline weight and blood pressure among groups (Figure S2A-C). The systolic blood pressure (SBP) change tendency was observed, and that SBP of mice developed a different sensitivity to sodium among groups (Figure 1A). Compared with the CON group, the blood pressure of the HS group significantly showed elevation from the 4th week. In contrast, the SBP of the PLR-H group was significantly lower compared to the HS group and maintained no difference from the CON group during the whole experiment. However, SBP in the PLR-L and PLR-M groups were not significantly different from that of the HS group at the end of the experiment. Further, changes in mean blood pressure (MBP) were not significantly different among groups (Figure S2D). The weight change tendency was also recorded, HS group gained weight more slowly and showed a significant difference in weight compared to those in the CON group from the 4th week onwards. PLR intervention could maintain a normal rate of weight gain to some extent, but there were no significant differences in their effects (Figure S2E). In the 8th week, we used serum creatinine, urine protein and kidney histologic stains to assess the extent of kidney damage as well as the efficiency of PLR on kidney protection. Compared with the CON group, the HS group showed significantly aggravated serum creatinine and urine protein (Figure 1B, C), however, these biochemical parameters were significantly improved in PLR-M and PLR-H groups. Moreover, the macroscopic pictures of kidneys of the PLR-M and PLR-H groups exhibited markedly less hyperemia and swelling compared with the HS and PLR-L groups (Figure 1D). Consistent with this appearance, the kidney coefficient, as well as histopathological injury observed by HE staining and proportion of fibrosis observed by MASSON staining was observably lower in the PLR-M and PLR-H groups than those in the HS group (Fig. 1E, F), whereas such histological coefficient differences did not indicate in liver and spleen among groups (Figure S2F, G). Notably, middle and high dose of PLR supplementation significantly alleviated CKD induced by chronic high salt diet. The PLR-H group better reduced the degree of fibrosis and renal HE scores compared to the PLR-M group. Taken

 doi:10.20944/preprints202401.0241.v1

together, we considered high dose of PLR was the most effective dose for CKD protection and evaluated it in the following experiment.

Compared with the CON group, the HS mice showed significantly upregulated mRNA levels of *Col1a1*, *Col3a1*, *TIMP-1* and *Fibronectin* (Figure 1G), which indicated fibrosis in kidneys of the HS group. Whereas high dose of PLR supplementation significantly downregulated these fibrosis related genes expression. In addition, the mRNA levels of *Kim-1* and *Ngal*, which indicated renal tubular injury, were markedly higher in the HS group than in the PLR-H group. Considering that the amount of salt intake could influence the severity of kidney injury, we compared total water intake and found the HS and all dose of PLR groups consumed similar amount of salt in the whole process of experiment (Figure S2H), also, both high salt intervention and high dose of PLR administration did not alter sodium loading as measured by urine and serum Na^+ (Figure 1H, I). In addition, concentrations of the other major ions in serum also have no differences among groups (Figure S2I, J).

3.2. PLR mitigated inflammatory response and down-regulated the Wnt / β-catenin pathway in kidney

To investigate the mechanisms by which high dose of PLR exerted its renoprotective effects, RNA-seq was performed to assessed gene expression profile of kidneys in the HS group versus the PLR-H group. Compared with the HS group, high dose of PLR administration altered the expression of 532 genes in kidney, with 53 transcripts being significantly upregulated and 479 being downregulated (Figure S2K). Gene set enrichment analyses (GSEA) based on GO and KEGG database were performed on the RNA-seq data and revealed that high dose of PLR substantially decreased the expression of genes related to the canonical Wnt signaling pathway (Figure 1K, L). Further, we found that high salt intake induced a significant increase in mRNA levels of *IL-6*, *TNF-α*, *CCL2* and *CCL3* in kidney (Figure 1J), and this effect was reversed by PLR-H group. To further verify whether the protective effect of high dose of PLR is related to Wnt / β-catenin pathway, we then detected the mRNA levels of molecules in Wnt signaling pathway. As presented in Figure 1M, high salt intake markedly increased *Wnt3* and *Wnt4* mRNA levels, the expression of β-catenin tended to increase in the HS group compared with the CON group, although no statistical difference was observed. Further, protein level of β-catenin was measured (Figure 1N, O), the expression level of which was significantly increased in the HS mice compared with the CON group, which demonstrated high salt intake could activate the canonical Wnt signaling pathway. While high dose of PLR administration could significantly down-regulate the mRNA and protein level of β-catenin, as well as the mRNA levels of *Wnt3* and *Wnt4*. In addition, TNF-α, which was able to induce β-catenin activation, its protein level was also found to be elevated in kidney tissue in HS group and reduced by high dose of PLR administration. Overall, we found that high dose of PLR could exert nephroprotective effects by down-regulating the expression of Wnt / β-catenin pathway.

Preprints (www.preprints.org) | NOT PEER-REVIEWED | Posted: 3 January 2024 doi:10.20944/preprints202401.0241.v1

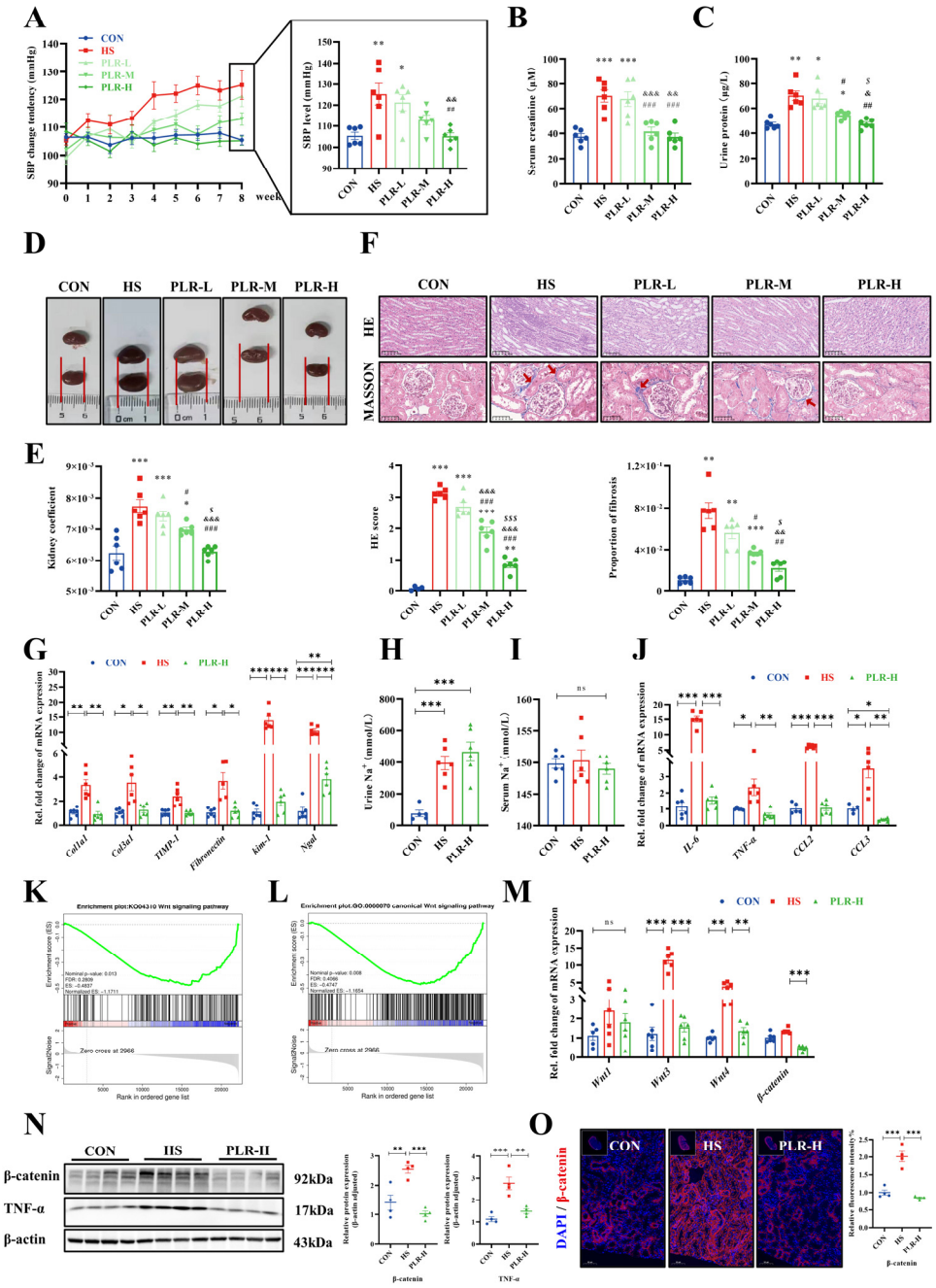

Figure 1. PLR alleviated kidney injuries induced by high salt diet and down-regulated the Wnt / β-catenin pathway in kidney of HS mice. (A) SBP change tendency of groups were evaluated noninvasively in the course of experiment. (B) Serum creatinine after 8 weeks. (C) Urine protein after 8 weeks. (D) Representative gross anatomy pictures of the kidney. (E) Kidney coefficient. (F) HE and MASSON staining of the kidney and the pathology scores and histological analysis. HE staining scale bar = 100 μm, MASSON staining scale bar = 50 μm. (G) RT-qPCR analysis of kidney injuries related genes. (H) Urine Na^+ concentration. (I) Serum Na^+ concentration. (J) RT-qPCR analysis of inflammatory factors genes in kidney. (K, L) GSEA performed on the RNA seq data (n = 3). (M) RT-qPCR analysis of Wnt1, Wnt3, Wnt4 and β-catenin genes in kidney (n = 5-6). (N) β-catenin and TNF-α protein levels in the kidney (n = 4). (O) Representative in situ detection of β-catenin in renal cortex was measured by immunofluorescent staining. Kidney tissue sections were stained with DAPI (blue) and probed with β-catenin (red). Scale bar = 50 μm (n = 4). Results are expressed as the mean ± SEM. n = 6 for each group. * p<0.05, ** p<0.01 and *** p<0.001, versus the CON group. # p<0.05, ## p<0.01 and

 doi:10.20944/preprints202401.0241.v1

$p<0.001$, versus the HS group. & $p<0.05$, && $p<0.01$ and &&& $p<0.001$, versus the PLR-L group. $ $p<0.05$, $$ $p<0.01$ and $$$ $p<0.001$, versus the PLR-M group in A-E. ***$p<0.001$, **$p<0.01$, *$p<0.05$ in G-J, M-O. PLR, Puerariae lobatae Radix; HS, high salt; SBP, systolic blood pressure; HE, hematoxylin-eosin; RT-qPCR, real-time quantitative PCR, GSEA, gene-set enrichment analyses.

3.3. PLR reduced intestinal inflammation and protected against intestinal barrier damage

Maternal intestinal damage, including inflammation and concomitant increased gut permeability, are involved in many extraintestinal disease including CKD. We hence examined the intestinal alterations, as shown in Figure 2A, compared with the HS group, PLR-H group relieved colon shortening to some extent, although no statistical difference was observed, which indicated that high dose of PLR intervention might alleviate colon inflammation. To further assess inflammation level, pro-inflammatory cytokines in colonic tissues were measured (Figure 2B). The mRNA levels *IL-6*, *CXCL1* and *CCL2* in the HS group were markedly higher, whereas the mRNA level of inflammatory protective factor *IL-10* was reduced compared with those in the CON group. However, the high dose of PLR supplementation significantly inhibited the expression of pro-inflammatory factors. In Figure 2C, a L-012 chemiluminescent probe was used to assess intestinal reactive oxygen species (ROS) *in vivo*[25]. The images indicated that chronic high salt intervention drastically elevated the concentration of ROS in the colon of mice, with significantly increased total flux in photons, while such an elevation was markedly dampened by high dose of PLR administration.

To further demonstrate the role of PLR administration in intestinal protection, intestinal tight junction markers in the colon were measured. Compared with the CON group, the HS group significantly downregulated mRNA levels of tight junction proteins, whereas the serum TNF-α level, LPS level and FD-4 permeability were elevated (Figure 2D-F). Moreover, the HS mice presented significantly deteriorative histopathological injury in the colon observed by HE staining, as well as decreased protein levels of ZO-1, Occludin and Claudin-1 observed by immunohistochemical staining and western blot (Figure 2G-J). However, all the above-mentioned damages induced by high salt were largely attenuated by high dose of PLR administration. Collectively, the above results demonstrated that therapeutic high dose of PLR administration alleviated intestinal inflammation as well as reinforced gut barrier.

Preprints (www.preprints.org) | NOT PEER-REVIEWED | Posted: 3 January 2024 doi:10.20944/preprints202401.0241.v1

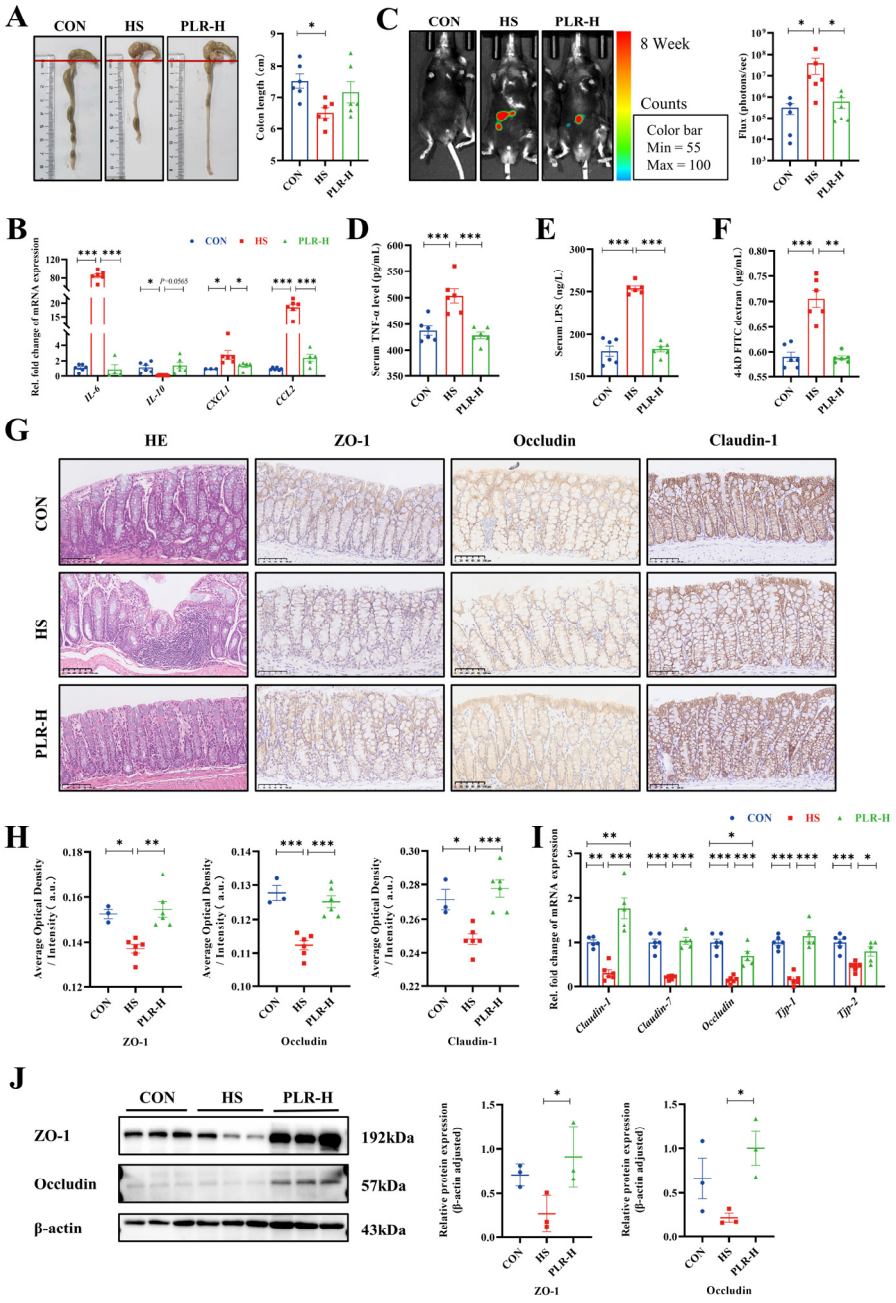

Figure 2. PLR reduced intestinal inflammation and protected against intestinal barrier damage in HS mice. (A) Representative gross anatomy pictures of the colon and the colon length measurement. (B) RT-qPCR analysis of inflammatory factors genes in colon. (C) Representative L-012 fluorescent staining and animal fluorescence imaging (n = 5-6). (D, E) Relative serum TNF-α and LPS level. (F) FD-4 level in the plasma. (G, H) HE staining and ZO-1, Occludin and Claudin-1 immunohistochemical staining in colon tissues. Scale bar = 100 μm (n = 3-6). (I) RT-qPCR analysis of tight junction proteins genes in colon (n = 5-6). (J) ZO-1 and Occludin protein levels in the colon (n = 3). Results are expressed as the mean ± SEM. n = 6 for each group. ***p<0.001, **p<0.01, *p<0.05 were determined by One-way ANOVA. LPS, lipopolysaccharide; FD-4, FITC-dextran 4-KD; HE, hematoxylin-eosin.

 doi:10.20944/preprints202401.0241.v1

3.4. PLR reversed gut microbial dysbiosis and increased the relative abundance of beneficial bacteria

The pathophysiological change of colon is always associated with enteric dysbiosis[27,28]. We further examined the impact of high dose of PLR on the gut microbiota composition and equilibrium via 16S rDNA sequencing. The relative abundance of *Firmicutes* as well as the *Firmicutes* / *Bacteroidetes* ratio in the cecal content of HS mice were lower than those in the cecal content of CON mice, whereas the level of *Bacteroidetes* was much higher in HS group (Figure S3A), which indicated that the microbial equilibrium was broken by chronic high salt feeding. However, high dose of PLR intervention reversed the dominant position of *Bacteroidetes* and upregulated the *Firmicutes* / *Bacteroidetes* ratio. In addition, the bacterial composition in cecal content samples from the three groups in terms of both bacterial phyla and genera were of significant differences (Figure 3A and Figure S3B). At the phylum level, *Verrucomicrobia* was the predominant phylum in PLR-H group compared with the HS group. At the genus level, the fecal microbiota was dominated by *Lachnospiraceae_NK4A136_group*, *Akkermansia* and *Lactobacillus*. Besides, different abundances of fecal bacterial taxa in the three groups were identified by LEfSe analysis (Figure 3B), which indicated that seven bacterial genera including SCFA-producing bacteria, such as *Akkermansia* and *Bifidobacterium* were enriched by high dose of PLR, while the other eight taxa, including *Rikenella, Prevotellaceae_UCG-001 and Lachnoclostridium* were enriched in the HS group (linear discriminant analysis [LDA] score > 3). Moreover, indicator species analysis showed a statistically significant higher relative abundance of *Faecalibaculum* and *Akkermansia* at the genus level in the PLR-H group than in the HS group (Figure 3C). We also found that *Lactobacillus* and *Bifidobacterium* also showed an increasing trend after high dose of PLR administration compared with the HS group. Additionally, the microbial dysbiosis index (MDI) showed an increased value in HS mice (Figure 3D), which was reversed by high dose of PLR intervention, indicating its reversion ability towards enteric dysbiosis.

In our study, alpha diversity was impacted by neither HS nor PLR-H administration (Figure S3C). However, Nonmetric multidimensional scaling (NMDS) and principal coordinate analysis (PCoA) showed that the overall structure of the gut microbiota was significantly different among the three groups (Figure 3E, F), in either beta diversity analysis, the HS group was significantly separated from the CON group, while the PLR-H group showed clustering overlap with the CON group. Indicating that the gut microbiota structure in HS mice was markedly influenced and shifted closer towards CON group by high dose of PLR intervention.

Further, spearman correlation analysis was performed (Figure 3G and Figure S3D). The relative abundance of *Akkermansia*, *Lactobacillus* as well as *Bifidobacterium* were negatively correlated with kidney injury related parameters and the Wnt / β-catenin signaling pathway transcripts, while positively correlated with tight junction proteins in colon. Relative abundance of these beneficial bacteria was also negatively correlated with inflammatory factors not only in colon but in kidney as well. In contrast, relative abundance of dominant bacteria (e.g., *Rikenella*, *Prevotellaceae_UCG-001* and *Lachnoclostridium*) in the HS group had a strong positive correlation with severity of injuries in colon and kidney.

Tax4Fun prediction analysis was then used to annotate the 16S rDNA data with metabolic pathways from the KEGG database (Figure 3H). The relative abundance of metabolism-associated signal transduction pathway showed a significant downregulate of Wnt signaling pathway in the PLR-H group compared with the HS group, which was in consistent with above mentioned pathway about the protective role of high dose of PLR in kidney injury. Also, VEGF signaling pathway, which was proven by previous studies to promote fibrosis in CKD[29], was lower in the PLR-H group than those in the HS group, suggesting that fibrotic signaling pathways were suppressed by high dose of PLR supplementation.

Above all, PLR administration could rectify gut microbiota dysbiosis and enhance the relative abundances of beneficial bacteria in mice, which were significantly negatively correlated with the severity of CKD.

Preprints (www.preprints.org) | NOT PEER-REVIEWED | Posted: 3 January 2024 doi:10.20944/preprints202401.0241.v1

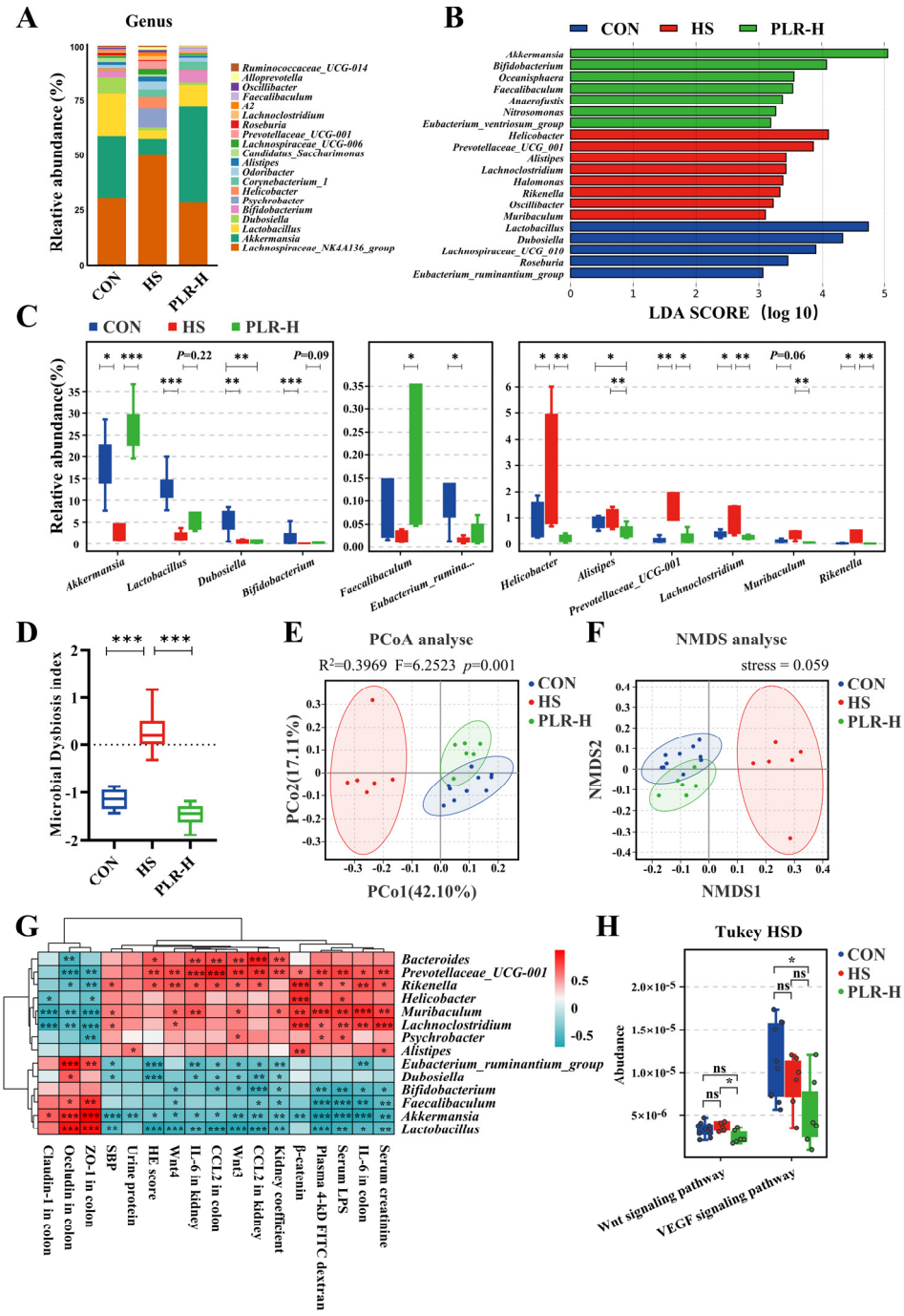

Figure 3. PLR reversed intestinal microbial dysbiosis in HS mice and remodeled gut microbiota by increase the relative abundance of probiotics. (A) Relative bacterial abundance at the genus level in the feces of mice. (B) Histogram of the LDA score showing the biomarker at the genus level of each group. (C) Relative abundance of indicator species at the genus level showing the enriched bacteria in the gut microbiome among groups. (D) Microbial Dysbiosis index of each group. (E, F) PCoA and NMDS based on the weighted UniFrac analysis of operational taxonomic units (OTUs). (G) Correlation heatmap of major indicator species and biomarkers based on LDA score and major injury indicators. (H) KEGG pathway analysis of function distribution and difference analysis based on Tax4Fun prediction results. Results are expressed as the mean ± SEM. n = 6-10 for each group. ***p<0.001, **p<0.01, *p<0.05 were determined by One-way ANOVA or Kruskal–Wallis test in C, D, adonis analysis and anosim analysis in E, Spearman analysis in G, Tukey HSD test in H. LDA, linear discriminant analysis; PCoA, principal coordinates analysis; NMDS, nonmetric multidimensional scaling; OTUs, operational taxonomic units; KEGG, kyoto encyclopedia of genes and genomes.

 doi:10.20944/preprints202401.0241.v1

3.5. Gut microbiota reestablished by PLR reduced renal tissue fibrosis and intestinal epithelial barrier impairment

Next, to confirm whether the protective effect of PLR against CKD was dependent on gut microbiome, we transplanted the gut microbiota derived from mice treated with PLR-H to CKD mice (Figure 4A). Baseline weight and blood pressure had no differences among groups (Figure S4A-C). Compared with the HS-FMT group, SBP, serum creatinine, together with urine protein, were significantly reduced in the PLR-FMT group (Figure 4B-D). As presented in Figure 4E, F and Figure S4D, the PLR-FMT group showed slighter macroscopic injury and lower kidney coefficient than HS-FMT group, however exhibited no statistical difference in liver and spleen coefficient among the three groups. As well, the kidney histopathological injury and fibrosis proportion were also reduced in the PLR-FMT group compared with the HS-FMT group (Figure 4G). Furthermore, the mRNA levels of inflammatory factors and chemokines, along with the mRNA levels of renal tubular related injury and interstitial fibrosis were also decreased in PLR-FMT group compared with the HS-FMT group (Figure 4H, I and Figure S4E). The above results indicated that bacteria deriving from the HS group could exacerbate the progression of CKD, however bacteria deriving from the PLR group could alleviate CKD damage.

In addition, we also explored the expression of Wnt / β-catenin pathway in kidney. As shown in Figure 4J, mRNA levels of *Wnt1*, *Wnt3*, *Wnt4* and *β-catenin* of the PLR-FMT group were lower than those in the HS-FMT group. Moreover, compared with the HS-FMT group, the protein levels of β-catenin as well as TNF-α were significantly reduced in the PLR-FMT group (Figure 4K-M). Taken together, these results suggested that the gut microbiota remodeled by PLR could protect kidney function, the effect of which probably associated with down-regulation of Wnt / β-catenin pathway.

Then we investigated whether gut microbiota from PLR was effective in alleviating inflammatory response of intestine and protecting intestinal barrier function. Colonic length was significantly reduced in the HS-FMT group compared to the CON group; however, this reduction was significantly mitigated by the intervention of PLR-derived gut microbiota and was restored to a length that was not significantly different from the CON group. Decreased mRNA levels of *IL-6*, *CXCL1* and *CCL2*, as well as increased *IL-10* mRNA expression in the colon were observed in the PLR-FMT group (Figure 5A, B) compared to the HS-FMT group, which indicated a lower colonic inflammatory environment generated by PLR-derived gut microbiota. Also, the bioluminescence imaging system exhibited images of less ROS in colonic tissues of the PLR-FMT group than the HS-FMT group (Figure 5C). Furthermore, HE staining of PLR-FMT colon showed less abscission and necrosis of epithelial cells, and less inflammatory cells infiltration compared with the HS-FMT group. All of which indicated the gut microbiota remodeled by PLR alleviated intestinal inflammation. As presented in Figure 5G-J, the mRNA and protein levels of ZO-1, Occludin and Claudin-1 in the colon were markedly higher, while the serum TNF-α level, LPS level and FD-4 permeability were significantly lower in the PLR-FMT group than those in the HS-FMT group (Figure 5D-F). These results suggested the HS-derived gut microbiota triggered gut permeability increasing and deteriorating intestinal barrier function, while the microbiota remodeled by PLR protected against colonic inflammation and intestinal barrier disruption, which reduced translocation of bacterial products and inflammatory cytokines into serum. The above results indicated that gut microbiota reestablished by PLR could reduce renal tissue fibrosis and colonic epithelial barrier damage.

Preprints (www.preprints.org) | NOT PEER-REVIEWED | Posted: 3 January 2024 doi:10.20944/preprints202401.0241.v1

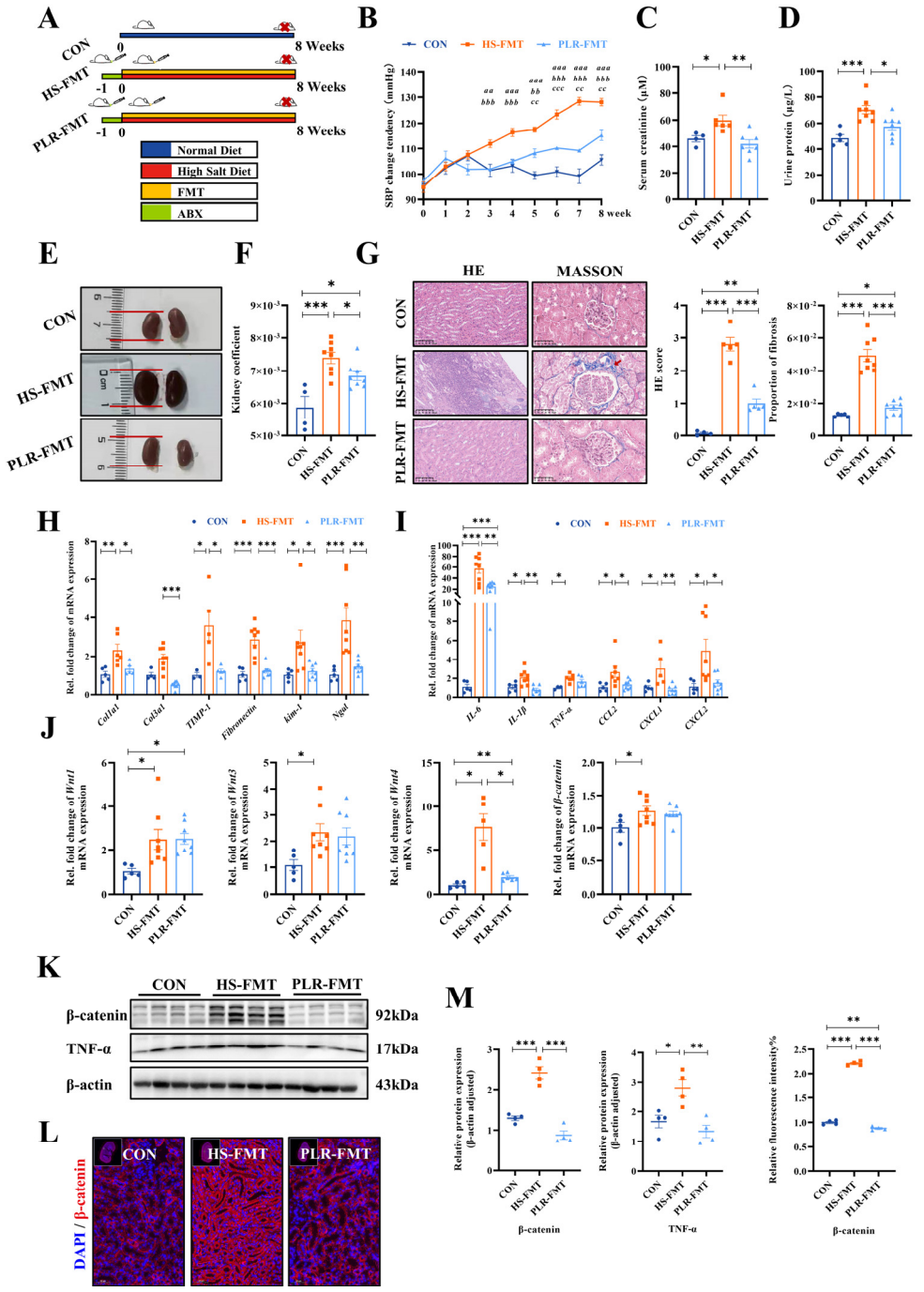

Figure 4. Gut microbiota from mice treated with PLR improved kidney tissue damage induced by high salt diet and down-regulated the Wnt / β-catenin pathway. (A) Flow chart of FMT experimental design. 8-week-old male C57BL/6 mice were given drinking water containing 2% w/v NaCl for 8 weeks. (B) SBP change tendency was evaluated noninvasively during experiment. *aa* indicates $p<0.01$ and *aaa* indicates $p<0.001$ for the CON group versus the HS-FMT group on the corresponding week. *bb* indicates $p<0.01$ and *bbb* indicates $p<0.001$ for the PLR-FMT group versus the HS-FMT group on the corresponding week. *cc* indicates $p<0.01$ and *ccc* indicates $p<0.001$ for the PLR-FMT group versus the CON group on the corresponding week. Repeated measurement ANOVA was used for statistical analysis. (C) Serum creatinine after 8 weeks. (D) Urine protein after 8 weeks. (E) Representative gross anatomy pictures of the kidney. (F) Kidney coefficient. (G) HE and MASSON staining of the kidney and the pathology scores and histological analysis. HE staining scale bar = 100 μm, MASSON staining

Preprints (www.preprints.org) | NOT PEER-REVIEWED | Posted: 3 January 2024 doi:10.20944/preprints202401.0241.v1

scale bar = 50 μm (n = 4-8). (H) RT-qPCR analysis of kidney injuries related genes. (I) RT-qPCR analysis of inflammatory factors genes in kidney. (J) RT-qPCR analysis of *Wnt1*, *Wnt3*, *Wnt4* and *β-catenin* genes in kidney (n = 5-8). (K-M) β-catenin and TNF-α protein levels in the kidney. Results are expressed as the mean ± SEM. n = 5-8 for each group. ***p<0.001, **p<0.01, *p<0.05 were determined by One-way ANOVA in C, D, F-I. PLR, Puerariae lobatae Radix; HS, high salt; FMT, fecal microbiota transplantation; ABX, antibiotic; SBP, systolic blood pressure; HE, hematoxylin-eosin; RT-qPCR, real-time quantitative PCR.

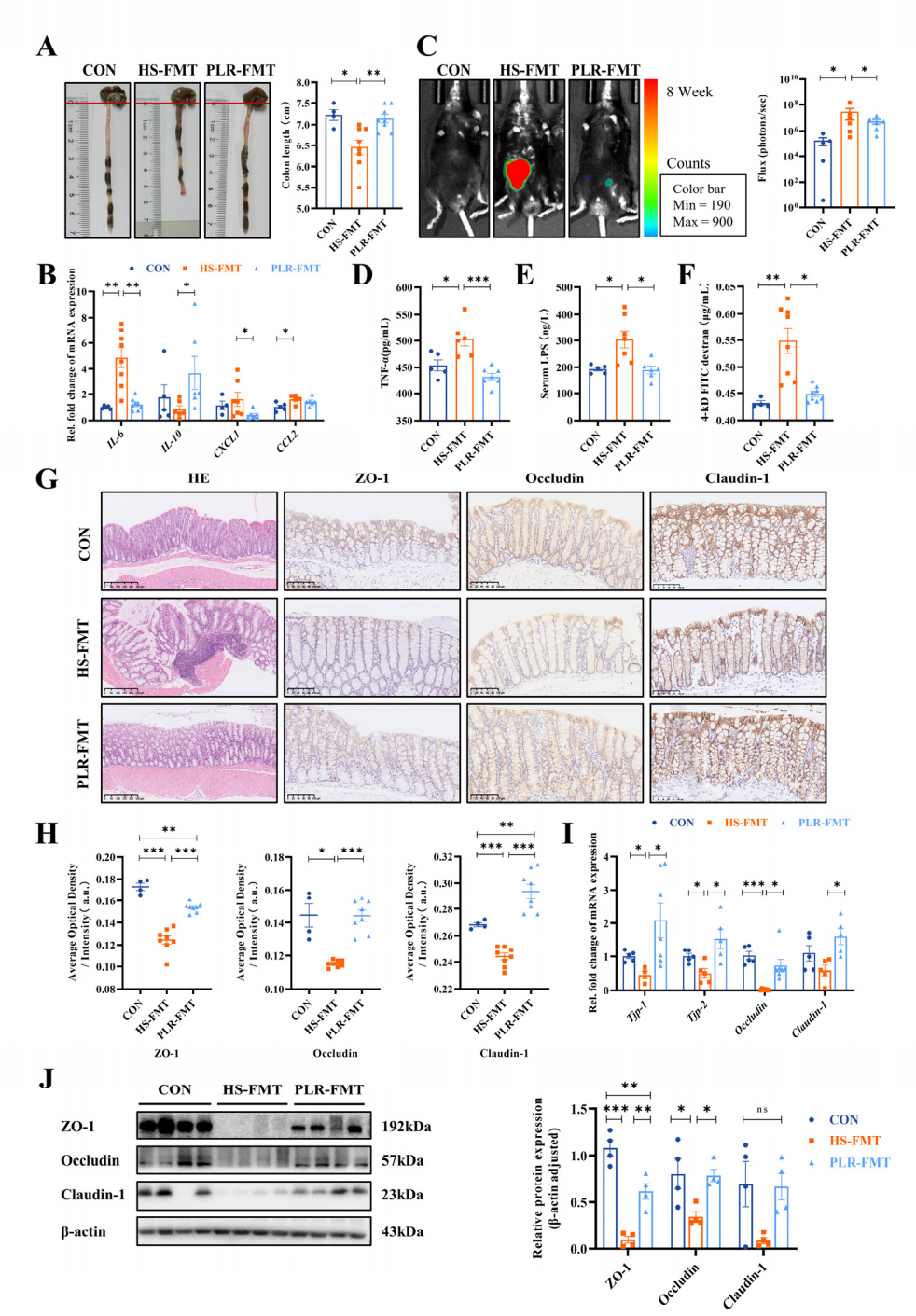

Figure 5. FMT from mice treated with PLR reduced intestinal inflammation and protected intestinal barrier function. (A) Representative gross anatomy pictures of the colon and the colon length measurement. (B) RT-qPCR analysis of inflammatory factors genes in colon. (C) Representative L-012 fluorescent staining and animal fluorescence imaging (n = 5-6). (D, E) Relative serum TNF-α and LPS level. (F) FD-4 level in the plasma. (G, H) HE staining and ZO-1, Occludin and Claudin-1

 doi:10.20944/preprints202401.0241.v1

immunohistochemical staining in colon tissues. Scale bar = 100 μm (n = 3-6). (I) RT-qPCR analysis of tight junction proteins genes in colon (n = 5-6). (J) ZO-1, Occludin and Claudin-1 protein levels in the colon (n = 4). Results are expressed as the mean ± SEM. n = 4-8 for each group. ***p<0.001, **p<0.01, *p<0.05 were determined by One-way ANOVA. LPS, lipopolysaccharide; FD-4, FITC-dextran 4-KD; HE, hematoxylin-eosin.

3.6. Gut microbiota rebuilt by PLR promoted intestinal homeostasis in CKD

To investigate the characteristic of gut microbiota that exerted renoprotective effects in FMT intervention, the microbial composition from HS-FMT group and PLR-FMT group were further analyzed. The main composition in either phylum or genus level was similar among groups (Figure 6A and Figure S5A). Notably, LEfSe analysis and indicator species analysis indicated that *Lactobacillus* and *Ruminococcaceae_UCG_014* at the genus level were significantly enriched by PLR-FMT (linear discriminant analysis [LDA] score > 3.6, Figure 6B, C), while the higher relative abundances of *Akkermansia* and *Bifidobacterium* were also found in PLR-FMT group. As shown in Figure S6A, the main composition in genus level was similar between the PLR-H group and the PLR-FMT group. Indicator species analysis revealed 111 shared genera species in the PLR-H and PLR-FMT group (Figure S6B). There were no significant differences in the relative abundance of major genera, such as *Dubosiella*, *Bifidobacterium*, *Psychrobacter*, and *Helicobacter* between the two groups, moreover, the relative abundance of *Akkermansia* and *Alistipes* in the PLR-FMT group was significantly lower than that of the PLR-H group, but the relative abundance of *Lactobacillus* and *Lachnoclostridium* was significantly higher than that of the PLR-H group (Figure S6C). Also, the increased value of MDI in HS-FMT mice was reversed by PLR-FMT intervention (Figure 6D). Though alpha diversity was not impacted by either HS-FMT or PLR-FMT administration (Figure S5B), PCoA analysis and NMDS showed that the gut microbiota structure was completely clustered (Figure 6E, F). Furthermore, spearman correlation analysis revealed that *Lactobacillus*, *Akkermansia* and *Ruminococcaceae_UCG_014*, which were enriched in PLR-FMT group, were significantly positively correlated with gut barrier related tight junction protein, while negatively correlated with damage related parameters and the Wnt signaling pathway related genes in kidney (Figure 6G). Finally, we explored different gut microbial metabolic function via Tax4Fun prediction analysis from KEGG data (Figure 6H and Figure S5C). The VEGF and Wnt signaling pathway were significantly downregulated in PLR-FMT mice compared with the HS-FMT group. Additionally, the tight junction about cell communication were higher in the PLR-FMT group compared with the other two groups in Tax4Fun prediction analysis, though no statistical difference was observed. This echoed previous results about the tight junction proteins in kidney and colon (Figure S4F, G), suggesting an increasing protective function of barriers in intestine and kidney after PLR-derived gut microbiota transplantation.

Overall, the aforementioned results indicated that FMT intervention could alter the structure of gut microbiota and the supplementary microbiota remodeled by high dose of PLR exerted a similar renoprotective effect similar as PLR-H group did. Further, *Lactobacillus*, *Akkermansia* and *Bifidobacterium* might be the dominating beneficial bacteria that both PLR-H and PLR-FMT group alleviated CKD.

Preprints (www.preprints.org) | NOT PEER-REVIEWED | Posted: 3 January 2024 doi:10.20944/preprints202401.0241.v1

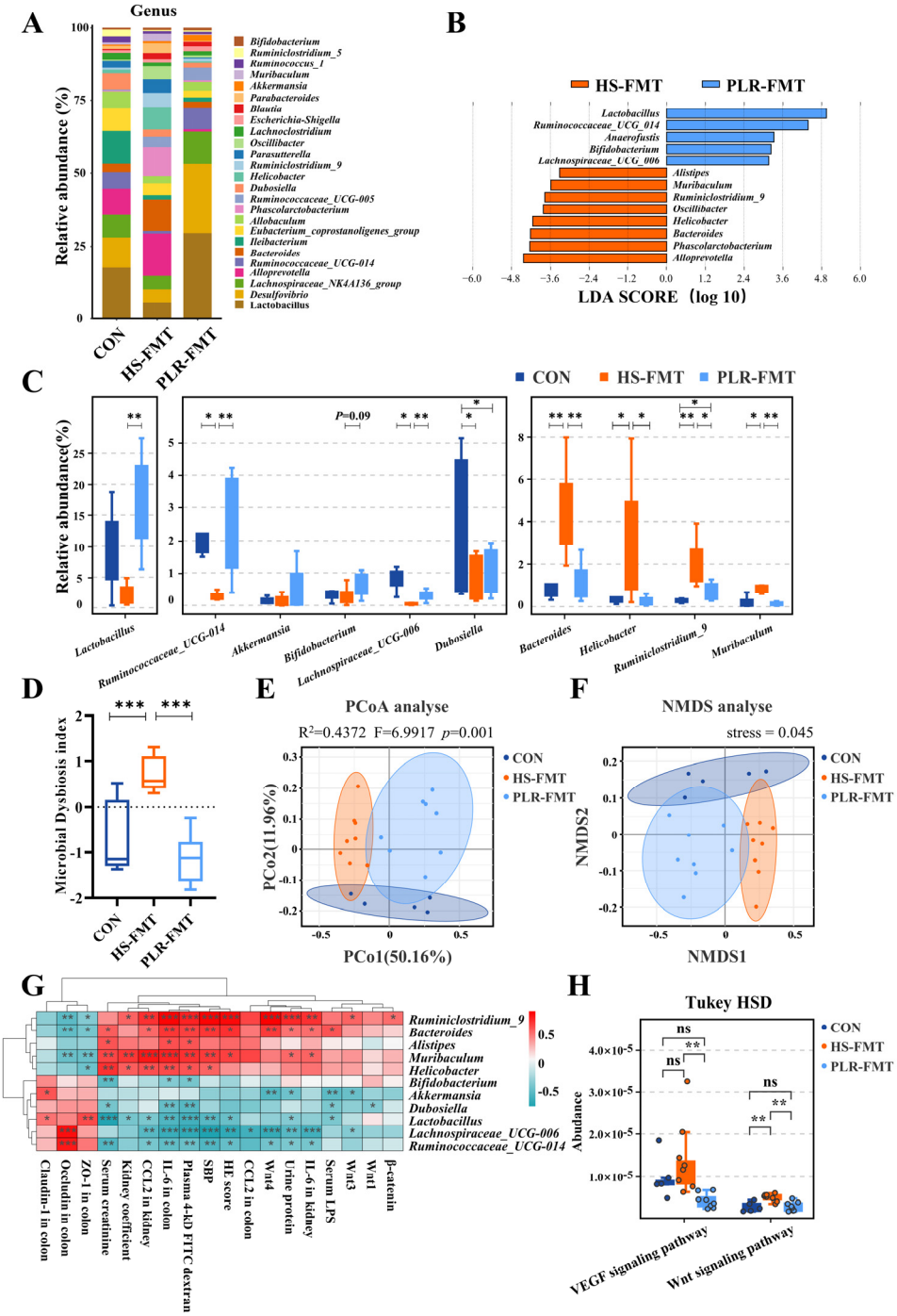

Figure 6. FMT from mice treated with PLR relieved intestinal microbial dysbiosis and rebuilt healthy microbiota environment. (A) Relative bacterial abundance at the genus level in the feces of mice. (B) Histogram of the LDA score showing the biomarker at the genus level between the HS-FMT group and the PLR-FMT group. (C) Relative abundance of indicator species at the genus level showing the enriched bacteria in the gut microbiome among groups. (D) Microbial Dysbiosis index of each group. (E, F) PCoA and NMDS based on the weighted UniFrac analysis of operational taxonomic units (OTUs). (G) Correlation heatmap of major indicator species and biomarkers based on LDA score and major injury indicators. (H) KEGG pathway analysis of function distribution and difference analysis based on Tax4Fun prediction results. Results are expressed as the mean ± SEM. n = 5-8 for each group. ***p<0.001, **p<0.01, *p<0.05 were determined by One-way ANOVA or Kruskal–Wallis test in C, D, adonis analysis and anosim analysis in E, Spearman analysis in G, Tukey HSD test in H. LDA, linear

 doi:10.20944/preprints202401.0241.v1

discriminant analysis; PCoA, principal coordinates analysis; NMDS, nonmetric multidimensional scaling; OTUs, operational taxonomic units; KEGG, kyoto encyclopedia of genes and genomes.

4. Discussion

It is well known that excessive salt intake is associated with hypertension, which closely links cardiovascular disease and CKD. Therefore, how to relieve the potential risk about kidney injury brought by high salt has arisen the attention[30,31]. Previous review advocated non-pharmacological strategies such as dietary and lifestyle modulation as well as kidney disease-specific pharmacological interventions to achieve kidney function preservation[32]. PLR is rich in nutrients including flavonoids, starch, saponins, and amino acids, and has always been a medicine and food homologous herb to relieve gastrointestinal and cardiovascular diseases[13]. PLR is consistent with the principles of the CKD management guidelines that advocate dietary control. However, whether PLR can have effect on CKD remains unclear. In the present study, for the first time, we found that oral PLR administration could alleviate CKD and the protective effect was achieved, at least partly by remodeling gut microbiota. Besides, PLR intervention significantly alleviated the renal fibrosis and down-regulated the canonical Wnt / β-catenin signaling pathway in kidney.

Salt is one of the most common dietary elements and plays an important role in maintaining the water-salt balance of the body. However excessive salt intake has been shown to associate with the development of cardiovascular diseases and other metabolic disease. In our study, prolonged excessive high salt diet led to gut microbiota disruption, intestinal inflammation, and permeability increasement. We found that high salt diet induced both inflammatory and fibrotic damage to the kidneys, probably because of harmful bacterial metabolites, like LPS, and inflammatory factors, including TNF-α, originating from the gut entering the circulation and inducing damage to distant organs. However, the therapeutic intervention of PLR could protect against both intestinal and renal injury, which we hypothesized may be a result of its ability to reverse disturbances in gut microbiota. We also found that PLR intervention increased *Akkermansia*, *Lactobacillus* and *Bifidobacterium* and decreased *Rikenella*, *Prevotellaceae_UCG-001* and *Lachnoclostridium*. In recent years, many clinical studies have found that gut microbiota can mediate associations between the gut and other organs, such as “gut-brain axis”, “gut-kidney axis”, etc. This suggests that gut microbiota may be a potential target for intervention in abenteric disease progression. Indeed, we confirmed that PLR exerted efficacy at least partially through gut microbiota by FMT experiment. PLR greatly increased the relative abundance of beneficial bacteria such as *Akkermansia*. *Akkermansia muciniphila* (*A. muciniphila*) is considered one of the key players in colonic mucus-associated microbiota and is necessary for gut to produce mucus to maintain a healthy mucus layer and thickness of the intestinal wall[33,34]. Previous study has demonstrated that increased colonization of *A. muciniphila* in the colon of mice mitigated gut barrier leakage and blood endotoxemia in experimental colitis[35]. Furthermore, previous clinical research showed the relative abundance of *Akkermansia* in the CKD patients was significantly lower than that in healthy group[36]. In addition, *Akkermansia* may be the driving factor to influence butanoate and tryptophan metabolism to alleviate renal fibrosis in CsA-induced chronic nephrotoxicity mice model[37]. Further, oral gavage of mice with *A. muciniphila* protected against HFD/CCl4-induced liver and kidney fibrosis by modulating inflammatory response[38]. Moreover, *A. muciniphila* administration suppressed epithelial-mesenchymal transition and reduced renal interstitial fibrosis in 5/6 nephrectomy rats[39]. This suggested that besides repairing the intestinal barrier, *Akkermansia* was also closely related to alleviating the damage of CKD and renal fibrosis. Similarly, in our study, our results also revealed that the relative abundances of *Akkermansia* were negatively correlated with nephritic histopathological fibrotic degree and biochemical indexes of kidney injury. Therefore, we hypothesized that the alleviating effect of PLR on CKD and renal fibrosis may be associated with increased colonization of *Akkermansia* in the intestine.

The gut microbiota is a complex ecosystem in which various strains of bacteria can interact with each other through resource competition and nutrient symbiosis[13], besides the protective effect of a single bacterium, symbiotic relationship between beneficial bacteria in intestinal homeostasis maintenance and disease protection should not be overlooked as well[40]. In our study, we found

that PLR also increased the relative abundance of *Bifidobacterium* and *Lactobacillus*, which have already been used as industrial production probiotics[41], are capable of enhancing the intestinal mucus layer and goblet cell function thus protecting the integrity of the intestinal barrier[42,43]. Similarly, in our previous study, we found that PLR induced concomitant increases in *Akkermansia* and *Bifidobacterium* in the treatment of ischemic stroke[16], which led us to hypothesize that both *Akkermansia* and *Bifidobacterium* were biomarkers for the efficacy of the protective efficacy of PLR in CKD. In vitro experiments demonstrated that *A. muciniphila* can stimulate the growth and of change the gene expression profile of *Lactobacillus*[44,45]. Studies have also shown that *Bifidobacterium* and *Lactobacillus* have potential benefit to reduce levels of uraemic toxins and protect against CKD[46–48]. PLR is rich in macromolecules such as starch, cellulose, and lignin[40,49]. These macromolecules reached the colon and provided energy for the synergistic growth of carbohydrate-utilizing bacteria such as *Bifidobacterium* and *Lactobacillus*[13,50,51]. In addition, above mentioned probiotics, together with *Faecalibaculum*, which could be enriched by PLR intervention in our study, have been reported as short-chain fatty acids-producing bacteria[52–54], which could increase SCFAs production and thus create an anti-inflammatory and anti-oxidative environment in intestinal. Moreover, such non-inflammatory stable state reduced gut barrier damage and permeation of harmful metabolites into plasma, thus decreased the adverse impact on abenteric organs. Together, the gut microbiota molded by PLR, characterized by *Akkermansia*, *Bifidobacterium* and *Lactobacillus*, is a key factor in its enteroprotective and nephroprotective effects.

Continuous intake of high salt needed to be excreted in urine to maintain the balance of water-salt in the plasma, which might be a sustained stimulation towards kidney in urine production that caused pathological damage and fibrosis of the kidneys. The Wnt signaling pathway is more accepted to influence high salt-related CKD at present[55]. Previous literature indicated that transient activation of Wnt / β-catenin facilitates kidney tissue generation after acute kidney injury, whereas sustained activation stimulates kidney fibrosis in CKD[56]. With the presence of high salt load, mice presented with more fibrosis and upregulated of the Wnt / β-catenin signal in heart and kidney[57,58]. In the present study, the intervention of PLR significantly alleviated the degree of renal fibrosis in high salt induced CKD. More importantly, gene set enrichment analysis showed the downregulation of canonical Wnt signaling pathway in PLR group. This might explain a potential pathway by which the PLR protected kidney from fibrosis. In our study, we inspected the Tax4Fun prediction analysis from the KEGG database and found that the Wnt signaling pathway was correlated with gut microbial metabolism. Besides, our results showed that the expression of the Wnt / β-catenin pathway as well as the level of pathological damage in kidney were in significantly negative correlation with the relative abundance of beneficial bacteria increased by PLR intervention, such as *Akkermansia*, *Lactobacillus* and *Bifidobacterium*, which led us to hypothesize that the gut microbiota may be effective in regulating the expression of the Wnt signaling pathway and subsequently slow down the process of renal fibrosis. Many studies have found that the Wnt signaling pathway can be regulated by gut microbiota. Treatment of mice with *A. muciniphila* is reported to significantly suppress EMT and reduced renal interstitial fibrosis[39]. Furthermore, treatment of *Bifidobacterium bifidum* and *Lactobacillus gasseri* with quercetin could exert inhibition of the canonical Wnt / β-catenin signaling pathway to protect against colorectal cancer in mice[59]. Both PLR and PLR-FMT intervention could significantly downregulated the Wnt signaling pathway. From this we speculated that alterations in the Wnt signaling pathway and alleviation of renal fibrosis by PLR intervention was associated with gut microbiota and their metabolism. On the other hand, PLR is rich in flavonoids, such as puerarin and daidzin. Study showed that combined use of vitamin D and *Puerarin* protected against hepatic fibrosis probably via silencing the Wnt1 / β-catenin pathway[60]. This suggested that in addition to manipulating the gut microbiota, the nephroprotection of PLR may be partially attributed to the antifibrotic effects of its small molecule active ingredients.

Inflammation and other signaling pathways can also contribute to CKD. In our study, significantly elevated protein level of TNF-α was found in serum and kidney of CKD mice. Increased TNF-α is one of the upstream targets for triggering β-catenin activation in kidney[61,62], the

 doi:10.20944/preprints202401.0241.v1

reduction of β-catenin has been shown to result in a lower expressions of fibrosis markers including fibronectin, Col1a1 and Col3a1[63–66]. However, the elevation of TNF-α and β-catenin were significantly suppressed by the intervention of PLR in the present study. This added to the possible targets for PLR exerting its nephroprotective effects. In addition, VEGF signaling pathway was another pathway that could be downregulated by PLR intervention in our study. Previous studies have shown that many therapies targeted at HIF-1α/VEGF signaling pathway to relieve liver fibrosis[67,68]. VEGF signaling pathway was also reported to have synergistic effect with Wnt / β-catenin signaling pathway in angiogenesis and fibrosis[69,70]. In our study, they may have corporate effects on renal fibrosis after PLR intervention.

PLR, as a traditional Chinese medicine and food homologous herb, has multi-target and multi-pathway pharmacodynamic routes of action. In the present study, we confirmed that PLR could alleviate CKD by remodeling the gut microbiota, repairing intestinal epithelial barrier, and downregulating the Wnt signaling pathway in the kidney, we identified for the first time that PLR relieved high salt diet-induced CKD by modulating the gut-kidney axis. However, our study definitely has some limitations; this study focused on gut microbiota entirety and their beneficial effect on CKD, and single strains of bacteria were not accessed. In addition, we focused on Wnt1, Wnt3 and Wnt4 in the canonical Wnt / β-catenin signaling pathway, this did not mean the other Wnt gene have no influence[71]. Previous studies have revealed that upregulation of Wnt4 and Wnt5 gene could activate the noncanonical Wnt pathway in hepatic stellate cells of fibrotic livers[72]. Additionally, Wnt6 is involved in epithelialization and loss of Wnt6 expression contributes to tubular injury and fibrosis in animal models[73]. Also, it was certainly that the beneficial pharmaceutical effects of PLR must mediate through more than one mechanism, the RNA-seq results also showed a differential KEGG enrichment in HIF-1 signaling pathway, Ferroptosis and MAPK signaling pathway, the potential role of which cannot be completely ruled out is a major limitation of this study. In the future, more deep understanding about the remodeling ability of PLR towards gut microbiota should be further explored. Overall, our study provides evidence for new function of PLR on kidney protection and a novel direction for the treatment of kidney disease.

5. Conclusions

In a nutshell, oral delivery of PLR attenuates high salt induced CKD. And the impacts of PLR on the composition and interaction of gut microbiota play a significantly important role in its protective pharmaceutical effect towards kidney. Protecting against oxidative, inflammatory as well as barrier destruction of colon to decrease harmful bacterial products and inflammatory factor into the plasma, thus inhibiting activation of the canonical Wnt / β-catenin might be a potential mechanism for PLR to alleviate kidney injury in vivo. Our study provides a novel insight into PLR-mediated protection of kidney injury through the microbiota-dependent 'gut-kidney axis' and put forward a potential therapeutic and preventive strategy target for kidney injury intervention.

Supplementary Materials: The following supporting information can be downloaded at the website of this paper posted on Preprints.org, Table S1: Changes in the proportion of mobile phase; Table S2: Primer sequences for qPCR; Figure S1: Chromatographic peaks of PLR samples analyzed for composition by ultra performance liquid chromatography; Figure S2: Baseline measurement and change tendency of mice in the whole process of experiment; Figure S3: PLR affected the composition of gut microbiota in HS mice and reversed intestinal dysbacteriosis; Figure S4: Baseline measurement and change tendency of mice in the whole process of FMT experiment; Figure S5: FMT from mice treated with PLR affected the composition of gut microbiota in HS mice and reversed intestinal dysbacteriosis; Figure S6: FMT from mice treated with PLR affected the composition of gut microbiota.

Author Contributions: PW and JWX conceived, designed, and interpreted the study. JWX, ZRZ, YY and QS undertook the data acquisition and analysis. MX, ZRZ, BLW, PCH and ZYF were responsible for the comprehensive technical support. JZ and JWX were major contributors in writing the manuscript. JZ and PW contributed to the inspection of data and final manuscript. All authors have read and agreed to the published version of the manuscript.

Funding: This research was funded by funding from the National Natural Science Foundation of China (grant No.82173304 and No.82370782), the Natural Science Foundation of Guangdong Province (grant No. 2021A1515012262 and No. 2023A1515012565).

Institutional Review Board Statement: The animal study protocol was approved by the Institutional Animal Ethical Care Committee of Southern Medical University (Guangzhou, China), Reference number: NFYY-2021-0572.

Informed Consent Statement: Not applicable.

Data Availability Statement: Raw sequencing data associated with microbial analysis in this study are stored in Mendeley Data and the doi number: 10.17632/6bmm3mmtd5.1, All other data is contained in the main manuscript and supplementary files.

Acknowledgments: Not applicable.

Conflicts of Interest: The authors declare no conflict of interest.

References

1. Cockwell, P.; Fisher, L.-A. The Global Burden of Chronic Kidney Disease. *Lancet* **2020**, *395*, 662–664, doi:10.1016/S0140-6736(19)32977-0.
2. Garofalo, C.; Borrelli, S.; Provenzano, M.; De Stefano, T.; Vita, C.; Chiodini, P.; Minutolo, R.; De Nicola, L.; Conte, G. Dietary Salt Restriction in Chronic Kidney Disease: A Meta-Analysis of Randomized Clinical Trials. *Nutrients* **2018**, *10*, 732, doi:10.3390/nu10060732.
3. Kim, S.M.; Jung, J.Y. Nutritional Management in Patients with Chronic Kidney Disease. *Korean J Intern Med* **2020**, *35*, 1279–1290, doi:10.3904/kjim.2020.408.
4. Oppelaar, J.J.; Vogt, L. Body Fluid-Independent Effects of Dietary Salt Consumption in Chronic Kidney Disease. *Nutrients* **2019**, *11*, 2779, doi:10.3390/nu11112779.
5. Yu, H.C.; Burrell, L.M.; Black, M.J.; Wu, L.L.; Dilley, R.J.; Cooper, M.E.; Johnston, C.I. Salt Induces Myocardial and Renal Fibrosis in Normotensive and Hypertensive Rats. *Circulation* **1998**, *98*, 2621–2628, doi:10.1161/01.cir.98.23.2621.
6. Zhou, B.; Liu, Y.; Kahn, M.; Ann, D.K.; Han, A.; Wang, H.; Nguyen, C.; Flodby, P.; Zhong, Q.; Krishnaveni, M.S.; et al. Interactions between β-Catenin and Transforming Growth Factor-β Signaling Pathways Mediate Epithelial-Mesenchymal Transition and Are Dependent on the Transcriptional Co-Activator cAMP-Response Element-Binding Protein (CREB)-Binding Protein (CBP). *The Journal of Biological Chemistry* **2012**, *287*, 7026–7038, doi:10.1074/jbc.M111.276311.
7. Zmora, N.; Suez, J.; Elinav, E. You Are What You Eat: Diet, Health and the Gut Microbiota. *Nat Rev Gastroenterol Hepatol* **2019**, *16*, 35–56, doi:10.1038/s41575-018-0061-2.
8. He, F.J.; Tan, M.; Ma, Y.; MacGregor, G.A. Salt Reduction to Prevent Hypertension and Cardiovascular Disease: JACC State-of-the-Art Review. *J Am Coll Cardiol* **2020**, *75*, 632–647, doi:10.1016/j.jacc.2019.11.055.
9. Miranda, P.M.; De Palma, G.; Serkis, V.; Lu, J.; Louis-Auguste, M.P.; McCarville, J.L.; Verdu, E.F.; Collins, S.M.; Bercik, P. High Salt Diet Exacerbates Colitis in Mice by Decreasing Lactobacillus Levels and Butyrate Production. *Microbiome* **2018**, *6*, 57, doi:10.1186/s40168-018-0433-4.
10. Yan, X.; Jin, J.; Su, X.; Yin, X.; Gao, J.; Wang, X.; Zhang, S.; Bu, P.; Wang, M.; Zhang, Y.; et al. Intestinal Flora Modulates Blood Pressure by Regulating the Synthesis of Intestinal-Derived Corticosterone in High Salt-Induced Hypertension. *Circ Res* **2020**, *126*, 839–853, doi:10.1161/CIRCRESAHA.119.316394.
11. Hu, J.; Luo, H.; Wang, J.; Tang, W.; Lu, J.; Wu, S.; Xiong, Z.; Yang, G.; Chen, Z.; Lan, T.; et al. Enteric Dysbiosis-Linked Gut Barrier Disruption Triggers Early Renal Injury Induced by Chronic High Salt Feeding in Mice. *Exp Mol Med* **2017**, *49*, e370–e370, doi:10.1038/emm.2017.122.
12. Li, H.-B.; Xu, M.-L.; Xu, X.-D.; Tang, Y.-Y.; Jiang, H.-L.; Li, L.; Xia, W.-J.; Cui, N.; Bai, J.; Dai, Z.-M.; et al. Faecalibacterium Prausnitzii Attenuates CKD via Butyrate-Renal GPR43 Axis. *Circ. Res.* **2022**, *131*, e120–e134, doi:10.1161/CIRCRESAHA.122.320184.
13. Huang, L.; Liu, Z.; Wu, P.; Yue, X.; Lian, Z.; He, P.; Liu, Y.; Zhou, R.; Zhao, J. Puerariae Lobatae Radix Alleviates Pre-Eclampsia by Remodeling Gut Microbiota and Protecting the Gut and Placental Barriers. *Nutrients* **2022**, *14*, 5025, doi:10.3390/nu14235025.
14. Li, Q.; Liu, W.; Feng, Y.; Hou, H.; Zhang, Z.; Yu, Q.; Zhou, Y.; Luo, Q.; Luo, Y.; Ouyang, H.; et al. Radix Puerariae Thomsonii Polysaccharide (RPP) Improves Inflammation and Lipid Peroxidation in Alcohol and High-Fat Diet Mice by Regulating Gut Microbiota. *Int J Biol Macromol* **2022**, *209*, 858–870, doi:10.1016/j.ijbiomac.2022.04.067.

15. Zhang, S.-S.; Zhang, N.-N.; Guo, S.; Liu, S.-J.; Hou, Y.-F.; Li, S.; Ho, C.-T.; Bai, N.-S. Glycosides and Flavonoids from the Extract of Pueraria Thomsonii Benth Leaf Alleviate Type 2 Diabetes in High-Fat Diet plus Streptozotocin-Induced Mice by Modulating the Gut Microbiota. *Food Funct* **2022**, *13*, 3931–3945, doi:10.1039/d1fo04170c.
16. Chen, R.; Wu, P.; Cai, Z.; Fang, Y.; Zhou, H.; Lasanajak, Y.; Tang, L.; Ye, L.; Hou, C.; Zhao, J. Puerariae Lobatae Radix with Chuanxiong Rhizoma for Treatment of Cerebral Ischemic Stroke by Remodeling Gut Microbiota to Regulate the Brain-Gut Barriers. *J Nutr Biochem* **2019**, *65*, 101–114, doi:10.1016/j.jnutbio.2018.12.004.
17. Avila-Carrasco, L.; García-Mayorga, E.A.; Díaz-Avila, D.L.; Garza-Veloz, I.; Martinez-Fierro, M.L.; González-Mateo, G.T. Potential Therapeutic Effects of Natural Plant Compounds in Kidney Disease. *Molecules (Basel, Switzerland)* **2021**, *26*, 6096, doi:10.3390/molecules26206096.
18. Zhou, Z.; Qiu, Y.; Li, K.; Sun, Q.; Xie, M.; Huang, P.; Yu, Y.; Wang, B.; Xue, J.; Zhu, Z.; et al. Unraveling the Impact of Lactobacillus Spp. and Other Urinary Microorganisms on the Efficacy of Mirabegron in Female Patients with Overactive Bladder. *Front. Cell. Infect. Microbiol.* **2022**, *12*, 1030315, doi:10.3389/fcimb.2022.1030315.
19. Qiu, Y.; Gao, Y.; Chen, C.; Xie, M.; Huang, P.; Sun, Q.; Zhou, Z.; Li, B.; Zhao, J.; Wu, P. Deciphering the Influence of Urinary Microbiota on FoxP3+ Regulatory T Cell Infiltration and Prognosis in Chinese Patients with Non-Muscle-Invasive Bladder Cancer. *Human Cell* **2022**, *35*, 511–521, doi:10.1007/s13577-021-00659-0.
20. Caporaso, J.G.; Kuczynski, J.; Stombaugh, J.; Bittinger, K.; Bushman, F.D.; Costello, E.K.; Fierer, N.; Peña, A.G.; Goodrich, J.K.; Gordon, J.I.; et al. QIIME Allows Analysis of High-Throughput Community Sequencing Data. *Nat Methods* **2010**, *7*, 335–336, doi:10.1038/nmeth.f.303.
21. Segata, N.; Izard, J.; Waldron, L.; Gevers, D.; Miropolsky, L.; Garrett, W.S.; Huttenhower, C. Metagenomic Biomarker Discovery and Explanation. *Genome Biol* **2011**, *12*, R60, doi:10.1186/gb-2011-12-6-r60.
22. Aßhauer, K.P.; Wemheuer, B.; Daniel, R.; Meinicke, P. Tax4Fun: Predicting Functional Profiles from Metagenomic 16S rRNA Data. *Bioinformatics* **2015**, *31*, 2882–2884, doi:10.1093/bioinformatics/btv287.
23. Love, M.I.; Huber, W.; Anders, S. Moderated Estimation of Fold Change and Dispersion for RNA-Seq Data with DESeq2. *Genome Biol* **2014**, *15*, 550, doi:10.1186/s13059-014-0550-8.
24. Subramanian, A.; Tamayo, P.; Mootha, V.K.; Mukherjee, S.; Ebert, B.L.; Gillette, M.A.; Paulovich, A.; Pomeroy, S.L.; Golub, T.R.; Lander, E.S.; et al. Gene Set Enrichment Analysis: A Knowledge-Based Approach for Interpreting Genome-Wide Expression Profiles. *Proc Natl Acad Sci U S A* **2005**, *102*, 15545–15550, doi:10.1073/pnas.0506580102.
25. Wirtz, S.; Popp, V.; Kindermann, M.; Gerlach, K.; Weigmann, B.; Fichtner-Feigl, S.; Neurath, M.F. Chemically Induced Mouse Models of Acute and Chronic Intestinal Inflammation. *Nat Protoc* **2017**, *12*, 1295–1309, doi:10.1038/nprot.2017.044.
26. Manabe, E.; Ito, S.; Ohno, Y.; Tanaka, T.; Naito, Y.; Sasaki, N.; Asakura, M.; Masuyama, T.; Ishihara, M.; Tsujino, T. Reduced Lifespan of Erythrocytes in Dahl/Salt Sensitive Rats Is the Cause of the Renal Proximal Tubule Damage. *Sci Rep* **2020**, *10*, 22023, doi:10.1038/s41598-020-79146-9.
27. Yan, A.W.; Fouts, D.E.; Brandl, J.; Stärkel, P.; Torralba, M.; Schott, E.; Tsukamoto, H.; Nelson, K.E.; Brenner, D.A.; Schnabl, B. Enteric Dysbiosis Associated with a Mouse Model of Alcoholic Liver Disease. *Hepatology* **2011**, *53*, 96–105, doi:10.1002/hep.24018.
28. Yu, L.C.-H.; Shih, Y.-A.; Wu, L.-L.; Lin, Y.-D.; Kuo, W.-T.; Peng, W.-H.; Lu, K.-S.; Wei, S.-C.; Turner, J.R.; Ni, Y.-H. Enteric Dysbiosis Promotes Antibiotic-Resistant Bacterial Infection: Systemic Dissemination of Resistant and Commensal Bacteria through Epithelial Transcytosis. *Am J Physiol Gastrointest Liver Physiol* **2014**, *307*, G824-835, doi:10.1152/ajpgi.00070.2014.
29. Miao, C.; Zhu, X.; Wei, X.; Long, M.; Jiang, L.; Li, C.; Jin, D.; Du, Y. Pro- and Anti-Fibrotic Effects of Vascular Endothelial Growth Factor in Chronic Kidney Diseases. *Ren Fail* **2022**, *44*, 881–892, doi:10.1080/0886022X.2022.2079528.
30. Hosohata, K. Biomarkers of High Salt Intake. *Adv Clin Chem* **2021**, *104*, 71–106, doi:10.1016/bs.acc.2020.09.002.
31. Favero, C.; Giordano, L.; Mihaila, S.M.; Masereeuw, R.; Ortiz, A.; Sanchez-Niño, M.D. Postbiotics and Kidney Disease. *Toxins (Basel)* **2022**, *14*, 623, doi:10.3390/toxins14090623.
32. Kalantar-Zadeh, K.; Jafar, T.H.; Nitsch, D.; Neuen, B.L.; Perkovic, V. Chronic Kidney Disease. *Lancet* **2021**, *398*, 786–802, doi:10.1016/S0140-6736(21)00519-5.
33. Belzer, C.; de Vos, W.M. Microbes Inside--from Diversity to Function: The Case of Akkermansia. *The ISME journal* **2012**, *6*, 1449–1458, doi:10.1038/ismej.2012.6.
34. Lopez-Siles, M.; Enrich-Capó, N.; Aldeguer, X.; Sabat-Mir, M.; Duncan, S.H.; Garcia-Gil, L.J.; Martinez-Medina, M. Alterations in the Abundance and Co-Occurrence of Akkermansia Muciniphila and Faecalibacterium Prausnitzii in the Colonic Mucosa of Inflammatory Bowel Disease Subjects. *Front. Cell. Infect. Microbiol.* **2018**, *8*, 281, doi:10.3389/fcimb.2018.00281.

35. Wade, H.; Pan, K.; Duan, Q.; Kaluzny, S.; Pandey, E.; Fatumoju, L.; Saraswathi, V.; Wu, R.; Harris, E.N.; Su, Q. Akkermansia Muciniphila and Its Membrane Protein Ameliorates Intestinal Inflammatory Stress and Promotes Epithelial Wound Healing via CREBH and miR-143/145. *J. Biomed. Sci.* **2023**, *30*, 38, doi:10.1186/s12929-023-00935-1.
36. Li, F.; Wang, M.; Wang, J.; Li, R.; Zhang, Y. Alterations to the Gut Microbiota and Their Correlation With Inflammatory Factors in Chronic Kidney Disease. *Front Cell Infect Microbiol* **2019**, *9*, 206, doi:10.3389/fcimb.2019.00206.
37. Han, C.; Jiang, Y.-H.; Li, W.; Liu, Y. Astragalus Membranaceus and Salvia Miltiorrhiza Ameliorates Cyclosporin A-Induced Chronic Nephrotoxicity through the "Gut-Kidney Axis." *J Ethnopharmacol* **2021**, *269*, 113768, doi:10.1016/j.jep.2020.113768.
38. Keshavarz Azizi Raftar, S.; Ashrafian, F.; Yadegar, A.; Lari, A.; Moradi, H.R.; Shahriary, A.; Azimirad, M.; Alavifard, H.; Mohsenifar, Z.; Davari, M.; et al. The Protective Effects of Live and Pasteurized Akkermansia Muciniphila and Its Extracellular Vesicles against HFD/CCl4-Induced Liver Injury. *Microbiol Spectr* **2021**, *9*, e0048421, doi:10.1128/Spectrum.00484-21.
39. Pei, T.; Hu, R.; Wang, F.; Yang, S.; Feng, H.; Li, Q.; Zhang, J.; Yan, S.; Ju, L.; He, Z.; et al. Akkermansia Muciniphila Ameliorates Chronic Kidney Disease Interstitial Fibrosis via the Gut-Renal Axis. *Microb Pathog* **2023**, *174*, 105891, doi:10.1016/j.micpath.2022.105891.
40. Lian, Z.; Xu, Y.; Wang, C.; Chen, Y.; Yuan, L.; Liu, Z.; Liu, Y.; He, P.; Cai, Z.; Zhao, J. Gut Microbiota-Derived Melatonin from Puerariae Lobatae Radix-Resistant Starch Supplementation Attenuates Ischemic Stroke Injury via a Positive Microbial Co-Occurrence Pattern. *Pharmacol. Res.* **2023**, *190*, 106714, doi:10.1016/j.phrs.2023.106714.
41. Sarao, L.K.; Arora, M. Probiotics, Prebiotics, and Microencapsulation: A Review. *Crit Rev Food Sci Nutr* **2017**, *57*, 344–371, doi:10.1080/10408398.2014.887055.
42. Engevik, M.A.; Luk, B.; Chang-Graham, A.L.; Hall, A.; Herrmann, B.; Ruan, W.; Endres, B.T.; Shi, Z.; Garey, K.W.; Hyser, J.M.; et al. Bifidobacterium Dentium Fortifies the Intestinal Mucus Layer via Autophagy and Calcium Signaling Pathways. *mBio* **2019**, *10*, e01087-19, doi:10.1128/mBio.01087-19.
43. Wang, J.; Ji, H.; Wang, S.; Liu, H.; Zhang, W.; Zhang, D.; Wang, Y. Probiotic Lactobacillus Plantarum Promotes Intestinal Barrier Function by Strengthening the Epithelium and Modulating Gut Microbiota. *Front. Microbiol.* **2018**, *9*, 1953, doi:10.3389/fmicb.2018.01953.
44. B, W.; X, C.; Z, C.; H, X.; J, D.; Y, L.; X, Z.; J, L.; G, W.; S, F.; et al. Stable Colonization of Akkermansia Muciniphila Educates Host Intestinal Microecology and Immunity to Battle against Inflammatory Intestinal Diseases. *Experimental & molecular medicine* **2023**, *55*, doi:10.1038/s12276-022-00911-z.
45. Cozzolino, A.; Vergalito, F.; Tremonte, P.; Iorizzo, M.; Lombardi, S.J.; Sorrentino, E.; Luongo, D.; Coppola, R.; Di Marco, R.; Succi, M. Preliminary Evaluation of the Safety and Probiotic Potential of Akkermansia Muciniphila DSM 22959 in Comparison with Lactobacillus Rhamnosus GG. *Microorganisms* **2020**, *8*, 189, doi:10.3390/microorganisms8020189.
46. Wang, X.; Yang, S.; Li, S.; Zhao, L.; Hao, Y.; Qin, J.; Zhang, L.; Zhang, C.; Bian, W.; Zuo, L.; et al. Aberrant Gut Microbiota Alters Host Metabolome and Impacts Renal Failure in Humans and Rodents. *Gut* **2020**, *69*, 2131–2142, doi:10.1136/gutjnl-2019-319766.
47. Tian, N.; Li, L.; Ng, J.K.-C.; Li, P.K.-T. The Potential Benefits and Controversies of Probiotics Use in Patients at Different Stages of Chronic Kidney Disease. *Nutrients* **2022**, *14*, 4044, doi:10.3390/nu14194044.
48. Mitrović, M.; Stanković-Popović, V.; Tolinački, M.; Golić, N.; Soković Bajić, S.; Veljović, K.; Nastasijević, B.; Soldatović, I.; Svorcan, P.; Dimković, N. The Impact of Synbiotic Treatment on the Levels of Gut-Derived Uremic Toxins, Inflammation, and Gut Microbiome of Chronic Kidney Disease Patients-A Randomized Trial. *J Ren Nutr* **2022**, S1051-2276(22)00152-2, doi:10.1053/j.jrn.2022.07.008.
49. Yue, S.-Y.; Zhou, R.-R.; Nan, T.-G.; Huang, L.-Q.; Yuan, Y. [Comparison of Major Chemical Components in Puerariae Thomsonii Radix and Puerariae Lobatae Radix]. *Zhongguo Zhong Yao Za Zhi = Zhongguo Zhongyao Zazhi = China Journal of Chinese Materia Medica* **2022**, *47*, 2689–2697, doi:10.19540/j.cnki.cjcmm.20220117.202.
50. Miranda, P.M.; De Palma, G.; Serkis, V.; Lu, J.; Louis-Auguste, M.P.; McCarville, J.L.; Verdu, E.F.; Collins, S.M.; Bercik, P. High Salt Diet Exacerbates Colitis in Mice by Decreasing Lactobacillus Levels and Butyrate Production. *Microbiome* **2018**, *6*, 57, doi:10.1186/s40168-018-0433-4.
51. Luo, Y.; Xiao, Y.; Zhao, J.; Zhang, H.; Chen, W.; Zhai, Q. The Role of Mucin and Oligosaccharides via Cross-Feeding Activities by Bifidobacterium: A Review. *Int. J. Biol. Macromol.* **2021**, *167*, 1329–1337, doi:10.1016/j.ijbiomac.2020.11.087.
52. Wu, Z.; Huang, S.; Li, T.; Li, N.; Han, D.; Zhang, B.; Xu, Z.Z.; Zhang, S.; Pang, J.; Wang, S.; et al. Gut Microbiota from Green Tea Polyphenol-Dosed Mice Improves Intestinal Epithelial Homeostasis and Ameliorates Experimental Colitis. *Microbiome* **2021**, *9*, 184, doi:10.1186/s40168-021-01115-9.
53. Chen, R.; Xu, Y.; Wu, P.; Zhou, H.; Lasanajak, Y.; Fang, Y.; Tang, L.; Ye, L.; Li, X.; Cai, Z.; et al. Transplantation of Fecal Microbiota Rich in Short Chain Fatty Acids and Butyric Acid Treat Cerebral Ischemic Stroke by Regulating Gut Microbiota. *Pharmacol Res* **2019**, *148*, 104403, doi:10.1016/j.phrs.2019.104403.

54. Lee, J.; d'Aigle, J.; Atadja, L.; Quaicoe, V.; Honarpisheh, P.; Ganesh, B.P.; Hassan, A.; Graf, J.; Petrosino, J.; Putluri, N.; et al. Gut Microbiota-Derived Short-Chain Fatty Acids Promote Poststroke Recovery in Aged Mice. *Circ Res* **2020**, *127*, 453–465, doi:10.1161/CIRCRESAHA.119.316448.
55. Feng, Y.; Ren, J.; Gui, Y.; Wei, W.; Shu, B.; Lu, Q.; Xue, X.; Sun, X.; He, W.; Yang, J.; et al. Wnt/β-Catenin-Promoted Macrophage Alternative Activation Contributes to Kidney Fibrosis. *Journal of the American Society of Nephrology: JASN* **2018**, *29*, 182–193, doi:10.1681/ASN.2017040391.
56. Schunk, S.J.; Floege, J.; Fliser, D.; Speer, T. WNT-β-Catenin Signalling - a Versatile Player in Kidney Injury and Repair. *Nat Rev Nephrol* **2021**, *17*, 172–184, doi:10.1038/s41581-020-00343-w.
57. Yamamoto, M.; Takahashi-Yanaga, F.; Arioka, M.; Igawa, K.; Tomooka, K.; Yamaura, K.; Sasaguri, T. Cardiac and Renal Protective Effects of 2,5-Dimethylcelecoxib in Angiotensin II and High-Salt-Induced Hypertension Model Mice. *J Hypertens* **2021**, *39*, 892–903, doi:10.1097/HJH.0000000000002728.
58. Manning, J.A.; Shah, S.S.; Nikolic, A.; Henshall, T.L.; Khew-Goodall, Y.; Kumar, S. The Ubiquitin Ligase NEDD4-2/NEDD4L Regulates Both Sodium Homeostasis and Fibrotic Signaling to Prevent End-Stage Renal Disease. *Cell Death Dis* **2021**, *12*, 398, doi:10.1038/s41419-021-03688-7.
59. Benito, I.; Encío, I.J.; Milagro, F.I.; Alfaro, M.; Martínez-Peñuela, A.; Barajas, M.; Marzo, F. Microencapsulated Bifidobacterium Bifidum and Lactobacillus Gasseri in Combination with Quercetin Inhibit Colorectal Cancer Development in ApcMin/+ Mice. *Int J Mol Sci* **2021**, *22*, 4906, doi:10.3390/ijms22094906.
60. Huang, G.-R.; Wei, S.-J.; Huang, Y.-Q.; Xing, W.; Wang, L.-Y.; Liang, L.-L. Mechanism of Combined Use of Vitamin D and Puerarin in Anti-Hepatic Fibrosis by Regulating the Wnt/β-Catenin Signalling Pathway. *World J Gastroenterol* **2018**, *24*, 4178–4185, doi:10.3748/wjg.v24.i36.4178.
61. Hiyama, A.; Yokoyama, K.; Nukaga, T.; Sakai, D.; Mochida, J. A Complex Interaction between Wnt Signaling and TNF-α in Nucleus Pulposus Cells. *Arthritis Res Ther* **2013**, *15*, R189, doi:10.1186/ar4379.
62. Zhao, Y.; Wang, C.; Hong, X.; Miao, J.; Liao, Y.; Hou, F.F.; Zhou, L.; Liu, Y. Wnt/β-Catenin Signaling Mediates Both Heart and Kidney Injury in Type 2 Cardiorenal Syndrome. *Kidney Int* **2019**, *95*, 815–829, doi:10.1016/j.kint.2018.11.021.
63. Pan, B.; Zhang, H.; Hong, Y.; Ma, M.; Wan, X.; Cao, C. Indoleamine-2,3-Dioxygenase Activates Wnt/β-Catenin Inducing Kidney Fibrosis after Acute Kidney Injury. *Gerontology* **2021**, *67*, 611–619, doi:10.1159/000515041.
64. Xiao, L.; Xu, B.; Zhou, L.; Tan, R.J.; Zhou, D.; Fu, H.; Li, A.; Hou, F.F.; Liu, Y. Wnt/β-Catenin Regulates Blood Pressure and Kidney Injury in Rats. *Biochim Biophys Acta Mol Basis Dis* **2019**, *1865*, 1313–1322, doi:10.1016/j.bbadis.2019.01.027.
65. Gelfand, B.D.; Meller, J.; Pryor, A.W.; Kahn, M.; Bortz, P.D.S.; Wamhoff, B.R.; Blackman, B.R. Hemodynamic Activation of Beta-Catenin and T-Cell-Specific Transcription Factor Signaling in Vascular Endothelium Regulates Fibronectin Expression. *Arterioscler Thromb Vasc Biol* **2011**, *31*, 1625–1633, doi:10.1161/ATVBAHA.111.227827.
66. Xiang, F.-L.; Fang, M.; Yutzey, K.E. Loss of β-Catenin in Resident Cardiac Fibroblasts Attenuates Fibrosis Induced by Pressure Overload in Mice. *Nat Commun* **2017**, *8*, 712, doi:10.1038/s41467-017-00840-w.
67. Lin, Y.; Dong, M.-Q.; Liu, Z.-M.; Xu, M.; Huang, Z.-H.; Liu, H.-J.; Gao, Y.; Zhou, W.-J. A Strategy of Vascular-Targeted Therapy for Liver Fibrosis. *Hepatology* **2022**, *76*, 660–675, doi:10.1002/hep.32299.
68. Sun, J.; Shi, L.; Xiao, T.; Xue, J.; Li, J.; Wang, P.; Wu, L.; Dai, X.; Ni, X.; Liu, Q. microRNA-21, via the HIF-1α/VEGF Signaling Pathway, Is Involved in Arsenite-Induced Hepatic Fibrosis through Aberrant Cross-Talk of Hepatocytes and Hepatic Stellate Cells. *Chemosphere* **2021**, *266*, 129177, doi:10.1016/j.chemosphere.2020.129177.
69. Jiang, L.; Yin, M.; Wei, X.; Liu, J.; Wang, X.; Niu, C.; Kang, X.; Xu, J.; Zhou, Z.; Sun, S.; et al. Bach1 Represses Wnt/β-Catenin Signaling and Angiogenesis. *Circ Res* **2015**, *117*, 364–375, doi:10.1161/CIRCRESAHA.115.306829.
70. Hung, S.W.; Zhang, R.; Tan, Z.; Chung, J.P.W.; Zhang, T.; Wang, C.C. Pharmaceuticals Targeting Signaling Pathways of Endometriosis as Potential New Medical Treatment: A Review. *Med Res Rev* **2021**, *41*, 2489–2564, doi:10.1002/med.21802.
71. Hong, F.; Hong, J.; Wang, L.; Zhou, Y.; Liu, D.; Xu, B.; Yu, X.; Sheng, L. Chronic Exposure to Nanoparticulate TiO2 Causes Renal Fibrosis Involving Activation of the Wnt Pathway in Mouse Kidney. *J Agric Food Chem* **2015**, *63*, 1639–1647, doi:10.1021/jf5034834.

72. Jiang, F.; Parsons, C.J.; Stefanovic, B. Gene Expression Profile of Quiescent and Activated Rat Hepatic Stellate Cells Implicates Wnt Signaling Pathway in Activation. *J Hepatol* **2006**, *45*, 401–409, doi:10.1016/j.jhep.2006.03.016.
73. Beaton, H.; Andrews, D.; Parsons, M.; Murphy, M.; Gaffney, A.; Kavanagh, D.; McKay, G.J.; Maxwell, A.P.; Taylor, C.T.; Cummins, E.P.; et al. Wnt6 Regulates Epithelial Cell Differentiation and Is Dysregulated in Renal Fibrosis. *Am J Physiol Renal Physiol* **2016**, *311*, F35-45, doi:10.1152/ajprenal.00136.2016.